A SEISMIC REFRACTION STUDY OF THE CRUSTAL STRUCTURE IN THE ACTIVE SEISMIC ZONE EAST OF TAIWAN

A THESIS SUBMITTED TO THE GRADUATE DIVISION OF THE
UNIVERSITY OF HAWAII IN PARTIAL FULFILLMENT
OF THE REQUIREMENTS FOR THE DEGREE OF

MASTER OF SCIENCE

IN GEOLOGY AND GEOPHYSICS

MAY 1987

By

Ricky Allen Hagen

Thesis Committee:

Frederick Duennebier, Chairman
Gerard Fryer
Patricia Fryer
Brian Taylor

We certify that we have read this thesis and that in our opinion it is satisfactory in scope and quality as a thesis for the degree of Master of Science in Geology and Geophysics.

THESIS COMMITTEE

____
Chairman

____

____

____

ACKNOWLEDGMENTS

I would like to especially thank Dr. Frederick Duennebier for providing moral and financial support during the course of this project. Fred's confidence and optimism kept me going many times when I might have faltered. Thanks are also due to Robert Cessaro for taking the time to help me along the path to computer literacy. Bob's programs, help, and advice saved me countless hours of work, and made this project a pleasant learning experience rather than a data processing nightmare.

Chip McCreery assisted in the data collection and provided assistance in the initial data reduction. Firmin Oliveira was responsible for much of the digitizing software (along with Bob Cessaro) and was often called upon for advice and assistance. Pat Cooper provided help with several programs that were used in the data analysis.

The data used in this study were collected by the officers and crew of R/V OCEAN RESEARCHER I under the direction of Dr. Vindell Hsu. Chip McCreery, Dave Barrett, and Marc Rosen handled the instrument preparation and assisted with the data collection.

This research was supported by the National Science Foundation, under NSF Grant OCE - 8410248.

ABSTRACT

During June and July 1985 an array of ten Hawaii Institute of Geophysics (HIG) ocean bottom seismometers (OBSs) was emplaced off the east coast of Taiwan. This experiment was part of a cooperative study conducted by scientists from HIG and Academia Sinica, Taiwan. As part of this experiment, three overlapping seismic refraction profiles were shot across the array parallel to the coast of Taiwan. The results of the raytrace modeling of these data indicate that the crust off southern and central Taiwan is oceanic. The crust was found to be about 8 km thick in this area and can be modeled by several layers with velocities and thicknesses that lie within the range associated with "normal" oceanic crust. Near 23.5° N a downwarping and thickening of the crustal layers occurs in the model. This downwarped trough of low-velocity materials may represent the sediment-filled axis of the Ryukyu Trench. If this is true, it indicates a more southerly trench position in this area than has been previously thought. To the north of this downwarping the bottom shoals rapidly and the velocity structure undergoes a transition that may indicate a change to arc or continental type crust.

TABLE OF CONTENTS

LIST OF TABLES

LIST OF ILLUSTRATIONS

INTRODUCTION

During June and July 1985 an array of ten Hawaii Institute of Geophysics (HIG) ocean bottom seismometers (OBSs) was emplaced off the east coast of Taiwan (Figure 1). This experiment was part of a cooperative study conducted by scientists from HIG and Academia Sinica, Taiwan. The OBSs were deployed from the R/V Ocean Researcher I, operated by Academia Sinica, and were recovered after a period of 32 days. The analog data cassettes were returned to HIG and processed into digital form for further study. The main purpose of this experiment was to improve the monitoring accuracy of the Taiwan Telemetered Seismic Network (TTSN) by placing OBSs to the east of the island, where better azimuthal coverage is needed to obtain more accurate hypocenter locations. The data collected by the OBS and TTSN arrays is being used to investigate the tectonic setting of the region east of Taiwan through seismicity and source mechanism studies (Hsu et al., 1986).

This paper will deal with the controlled source refraction shooting that was conducted to specific OBSs. This refraction data is modeled using a raytrace algorithm, to obtain the crustal velocity beneath the OBS array. The velocity structure obtained is then used in an attempt to resolve several questions about the nature of the plate boundaries in the tectonically complex area near Taiwan.

Figure 1

Bathymetric map of the area around Taiwan (Menard and Chase,1978). The OBS locations of this experiment are shown as black triangles. Contour interval = 200 fathoms.

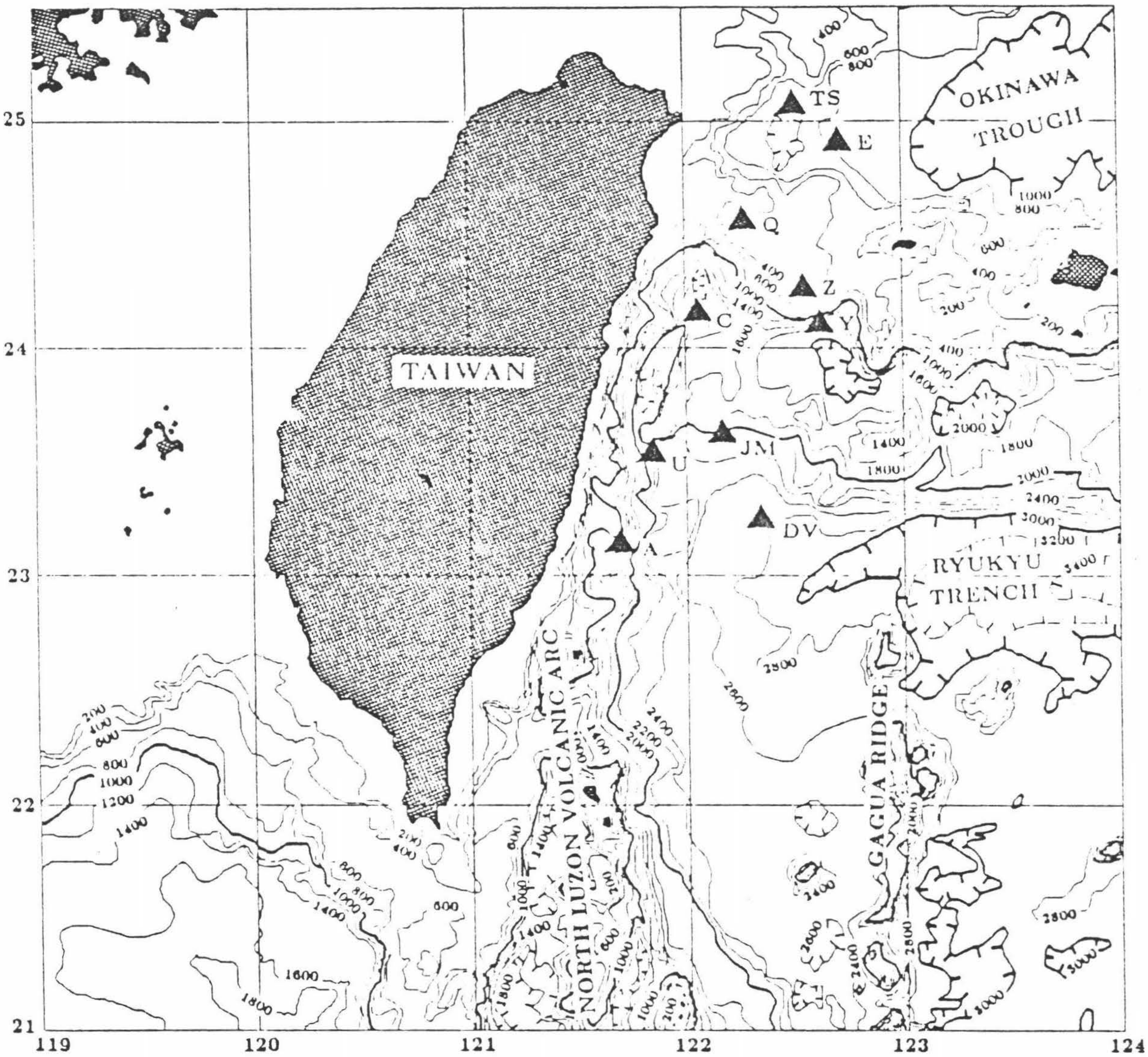
TAIWAN
OKINAWA TROUGH
RYUKYU TRENCH
NORTH LUZON VOLCANIC ARC
GAGUA RIDGE
TS
E
Q
Z
C
Y
JM
U
DV
A
25
24
23
22
21
119
120
121
122
123
124

TECTONIC SETTING

The tectonic setting of Taiwan is an unusual one in the island-arc systems of the western Pacific (Figure 2). The island of Taiwan formed as a result of the collision of the Philippine arc with the edge of the Eurasian plate beginning approximately 4 Ma in the early Pliocene (Karig, 1973; Wu, 1978; Letouzey and Kimura, 1985). Prior to this collision, eastward subduction of the oceanic crust of the South China Sea occurred beneath the northern Luzon arc. The collision resulted in compression, thickening, and uplift of the sediments of the Asiatic continental shelf to form the western part of Taiwan. The volcanic arc itself was then accreted to this wedge of sediments and forms the eastern Coastal Range of Taiwan.

The young orogenic belt of Taiwan consists of folded and faulted metamorphic basement rocks of Mesozoic age overlain by Tertiary sediments. These formations occur in long, narrow, NNE-trending belts. Nearly the entire section consists of a stack of folded, imbricate thrust sheets (Figure 3).

The Longitudinal Valley is a 150 km long, NNE-trending feature that separates the uplifted sedimentary sequence on the west from the volcanic arc sequence of the Eastern Coastal Range. The floor of the valley has a width of 5 to 7 km and is about 200 m above sea level. To the east side the Coastal Range reaches a height of about 1600 m while to the west the Central Range reaches 4000 m within 35 km of the valley. The Longitudinal Valley is believed to be the contact or suture zone between the sedimentary sequence of the continental margin

Figure 2

The plate tectonic setting of Taiwan (Ho,1986). The Philippine Sea plate is moving northwestward and subducting beneath the Ryukyu arc in the north and the Philippines in the west. The collision of the Luzon arc with the continental shelf is causing a complex collision zone to form around Taiwan.

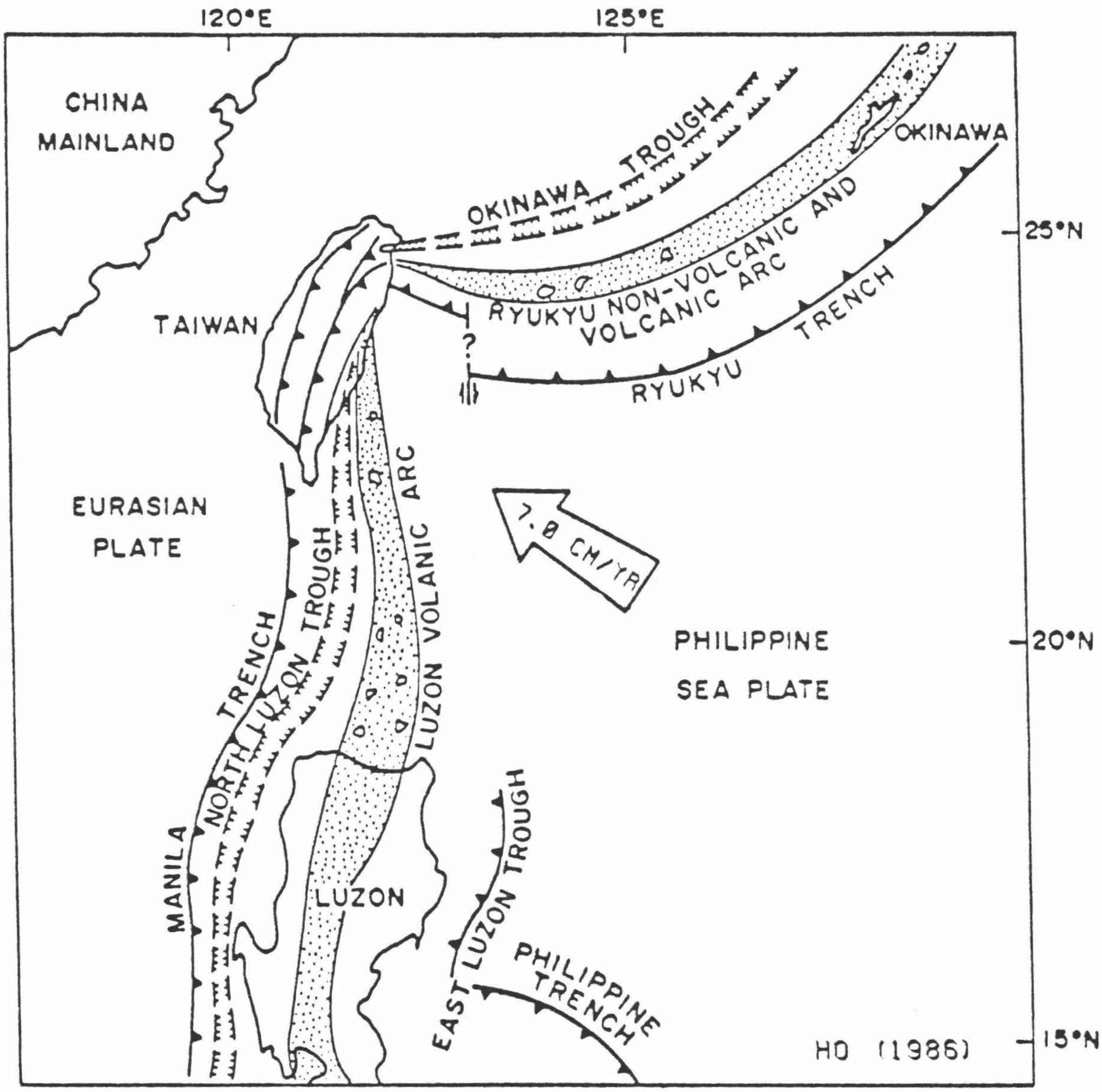
120°E
125°E
25°N
20°N
15°N
CHINA
MAINLAND
OKINAWA TROUGH
OKINAWA
RYUKYU NON-VOLCANIC AND
VOLCANIC ARC
RYUKYU TRENCH
TAIWAN
?
EURASIAN
PLATE
7.8 CM/YR
PHILIPPINE
SEA PLATE
MANILA TRENCH
NORTH LUZON TROUGH
LUZON VOLANIC ARC
LUZON
EAST LUZON TROUGH
PHILIPPINE TRENCH
HO (1986)

Figure 3

Tectonic/morphologic belts of Taiwan. The arc materials of the Coastal range are separated from the folded and faulted sedimentary and metamorphic rocks to the west by the Longitudinal Valley fault zone (LVFZ) (Ernst et al., 1985).

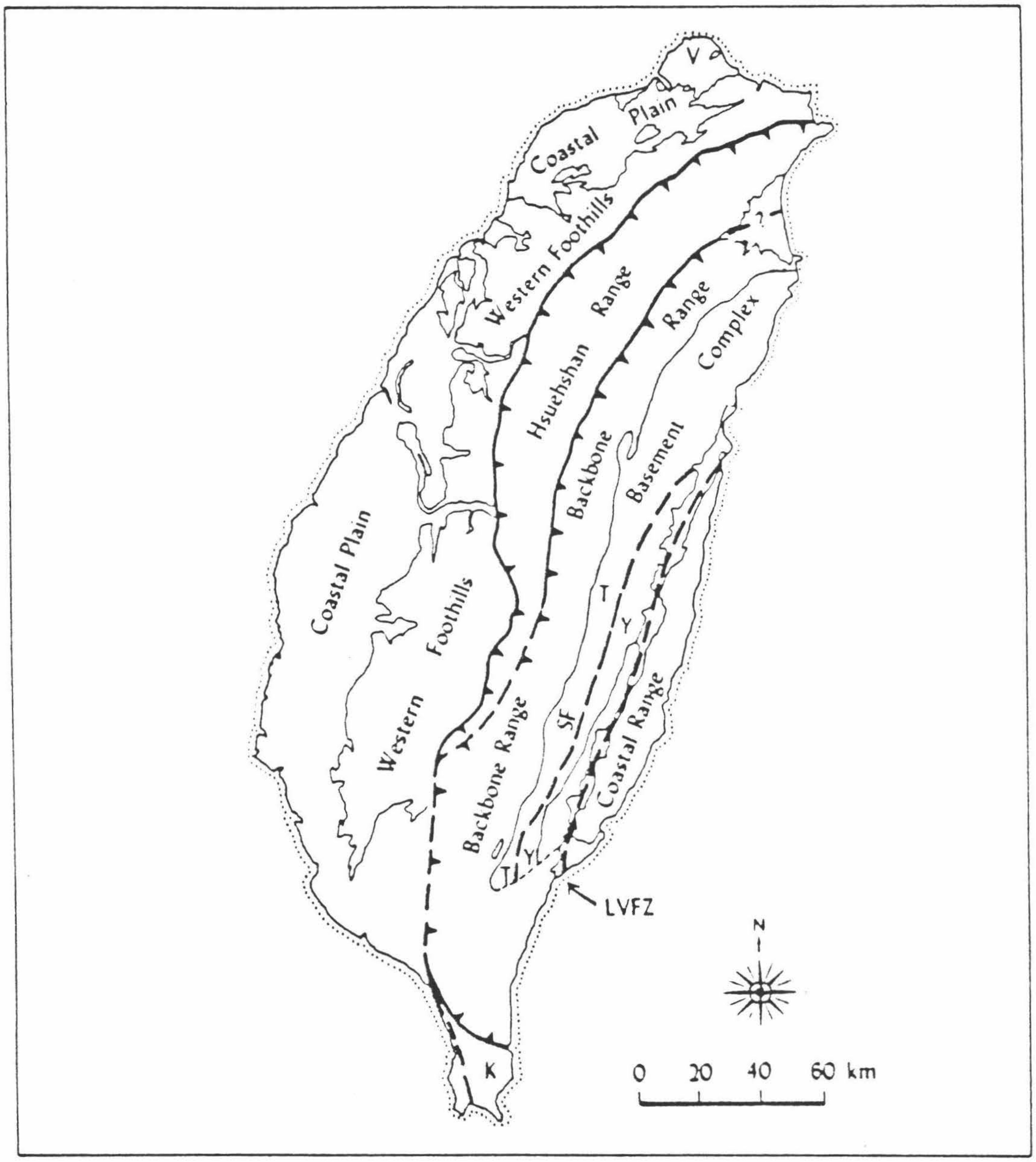
V
Coastal Plain
Western Foothills
Hsuehshan Range
Backbone Range
Basement Complex
Coastal Plain
Western Foothills
T
Y
SF
Backbone Range
Coastal Range
T
Y
LVFZ
K
N
0 20 40 60 km

and the volcanics of the Luzon arc (Juan, 1975; Lin and Tsai, 1978; Biq, 1981; Ho,1986).

To the south of Taiwan, eastward subduction of the South China Sea plate beneath the Philippines is occurring along the Manila Trench (Taylor and Hayes, 1983). The seismic evidence indicates that westward subduction is currently developing to the east of Luzon along the Philippine Trench and East Luzon Trough (Karig, 1973; Seno and Kurita, 1978; Lin and Tsai, 1981; Lewis and Hayes, 1983). Bowin et al. (1978) have suggested that the east-dipping subduction along the Manila Trench has been "sealing" southward from Taiwan as the more easily subducted crust of the South China Sea is consumed and the thicker crust of the continental shelf reaches the trench.

The Luzon volcanic arc extends from Luzon Island to Taiwan. Recent volcanic activity is confined to Luzon and the small islands between Luzon and Taiwan such as Batan and the Babuyan Islands. No active volcanoes are known in the Coastal Range of Taiwan where volcanism occurred during the late Miocene and Pliocene. This supports the hypothesis that collision, and the resulting cessation of volcanism, began in the northern arc in the Miocene and progressed southward to Luzon where volcanic activity continues today (Ernst et al., 1985).

The distribution of historical seismicity shows a gradual change as one moves north from Luzon towards Taiwan (Figure 4). The distribution of epicenters in central Luzon define a shallow (<200 km) east dipping Wadati-Benioff zone associated with subduction along the Manila Trench (Seno and Kurita, 1978; Wu, 1978; Lin and Tsai, 1981;

Figure 4

The distribution of seismicity (19 - 19) along the western margin of the Philippine Sea plate (Wu,1978).

SEISMICITY OF THE TAIWAN-PHILIPPINE REGION

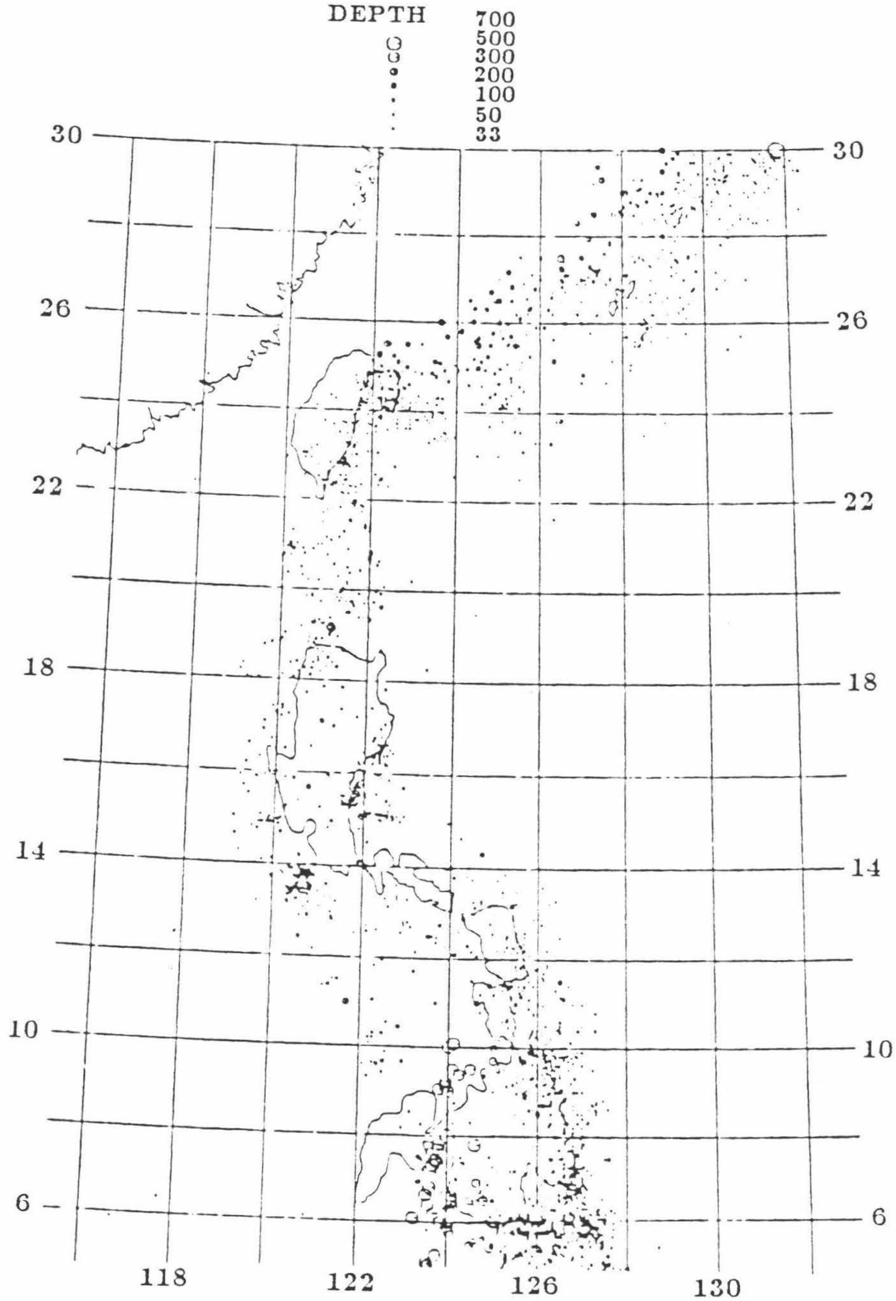

Hamburger et al., 1983). Moving further north, the western seismicity becomes shallower and more diffuse and an eastwardly dipping slab can no longer be defined.

The data also show a concentration of shallow events on the east side of Luzon that have thrust mechanisms. Although a subducting slab is not well defined by the seismicity, it is thought that subduction is beginning along the East Luzon Trough (Fitch, 1972; Wu, 1978; Seno and Kurita, 1978; Cardwell et al., 1980; Lin and Tsai, 1981). Lewis and Hayes (1983) collected several multichannel reflection profiles off eastern Luzon that clearly delineate the subducting plate and the deformation of the associated subduction complex. No compressive deformation was observed north of 18° N, where the eastern concentration of seismicity becomes more diffuse.

In the region between Luzon and Taiwan the seismicity is spread across a broad, shallow zone and includes both strike-slip and thrust events. Seno and Kurita (1978) proposed a model in which compression in this area is accommodated by left-lateral shear along NW-SE trending faults. However, Karig (1973) proposed that the arcuate NNE-SSW trending bathymetric troughs which cut the North Luzon Trough and the Luzon Arc represent the traces of active left-lateral faults. Karig's hypothesis is supported by Lewis and Hayes (1983) who interpret the bathymetry and seismicity to indicate that faulting is occurring along curvilinear north to northeast trending fault traces. Mrozowski et al. (1982) found that the basement structural fabric in the west Philippine basin is predominantly oriented NE-SW. This further supports the choice of the NE-trending nodal plane as the fault plane for the focal mechanisms in this area.

Beneath Taiwan the seismicity forms a shallow, diffuse zone concentrated along the eastern margin of the island (Wu, 1978; Tsai et al., 1977; Lin and Tsai, 1978; Lee, 1983). Off northeastern Taiwan the foci deepen to the north and merge into the events associated with the Ryukyu arc (Katsumata and Sykes, 1969; Tsai et al., 1977). Focal mechanism studies of the events beneath Taiwan indicate that the island is predominantly undergoing east-west compression with some left-lateral shear occurring along NNE-trending faults (Wu, 1970 and 1978; Lin and Tsai, 1981).

The earthquake data suggest that the convergence of the Eurasian and Philippine Sea plates is being accommodated in Taiwan by thrusting and left-lateral strike slip centered in the Longitudinal Valley area (Hsu, 1962; Wu, 1970; Seno and Kurita, 1978; Lee, 1983). One explanation for the tectonic complexity of the Taiwan area is that a broad zone of deformation, rather than a discrete plate boundary, has formed in Taiwan. Subduction and collision may be occurring in a belt over 100 km wide. This type of deformation zone may represent an early phase in the process of arc reversal (Ho, 1986).

To the northeast of Taiwan, northwestward subduction of the Philippine Sea plate is occurring beneath the Eurasian plate along the Ryukyu Trench. Convergence between the Philippine Sea Plate and the Eurasian plate is occurring in a NNW direction at a rate of 7 cm/yr (Seno, 1977). The Ryukyu arc is constructed on the Asiatic continental margin and is bounded by the active Okinawa Trough back-arc basin in the north and the Ryukyu Trench subduction zone in the south.

Back-arc rifting initiated in the Ryukyu volcanic arc during the late Miocene with a major phase of extension occurring in the south and central Okinawa Trough about 1.9 Ma (Kimura, 1985). The timing of the evolution of Taiwan and the opening of the southern Okinawa Trough suggests that rifting was the result of clockwise rotation and extension of the Eurasian plate caused by the collision of the Luzon arc with the continental margin (Letouzey and Kimura, 1985). Spreading is currently active in the south and central Okinawa Trough, at a rate of 2 to 3 cm/yr (Kimura, 1985), but the northern Okinawa Trough appears to be only in a rifting stage at the present time.

Recent volcanic activity along the Ryukyu arc occurs at a distance of between 160 to 250 km from the trench and is located 80 to 120 km above the Wadati-Benioff zone (Letouzey and Kimura,1985). Most of the recently active volcanoes of the arc are located in Kyushu and the northern part of the arc. In fact, only one Pleistocene arc volcanic center is located between Okinawa and Taiwan.

DATA COLLECTION AND REDUCTION

An array of ten Hawaii Institute of Geophysics (HIG) ocean bottom seismometers (OBSs) was emplaced off the east coast of Taiwan during June and July 1985 in cooperation with scientists from Academia Sinica, Taiwan to monitor the seismicity of the area.

Due to severe weather conditions, the controlled source seismic refraction portion of the experiment was severely curtailed. Thirty-nine explosive shots, from 5 to 250 kg each, were fired for OBS location and as refraction sources. In addition a single line of airgun shots was run across five of the OBSs, parallel to the east coast of Taiwan, and perpendicular to the bottom structure as indicated by the bathymetry (Figure 5).

Each OBS continuously recorded four channels of data on analog tape cassettes: hydrophone, time code, 4.5 Hz horizontal geophone, and 4.5 Hz vertical geophone (Sutton et al., 1977; Byrne et al., 1983). Of the five OBSs located along the airgun line: OBS U suffered a deployment problem and recorded only poor quality geophone data (no hydrophone data) during the refraction experiment. OBS Q, located at a very shallow depth, suffered from extreme ocean current noise. As a result only OBS TS, OBS C, and OBS A returned refraction data that were considered good enough for this study.

After retrieval of the instruments the data were adjusted for any tape skew errors incurred in the recording process and digitized onto computer tape. A correction was subsequently made for any drift of the OBS and ship clocks from the WWV standard. Navigation during the experiment was based on transit satellite fixes and radar fixes to Taiwan shore stations. Navigational accuracy was variable during the experiment, but the average navigational error is estimated to be less than 0.3 km. Relative shot and receiver locations were determined by a generalized inversion of direct water-wave travel times using a method that is similar to an earthquake location algorithm, but in which both

Figure 5

Bathymetric map of the experiment area showing the locations of the OBSs (triangles), explosive shots (dots), and the refraction lines used in this study (patterns). Contour interval = 200 fathoms.

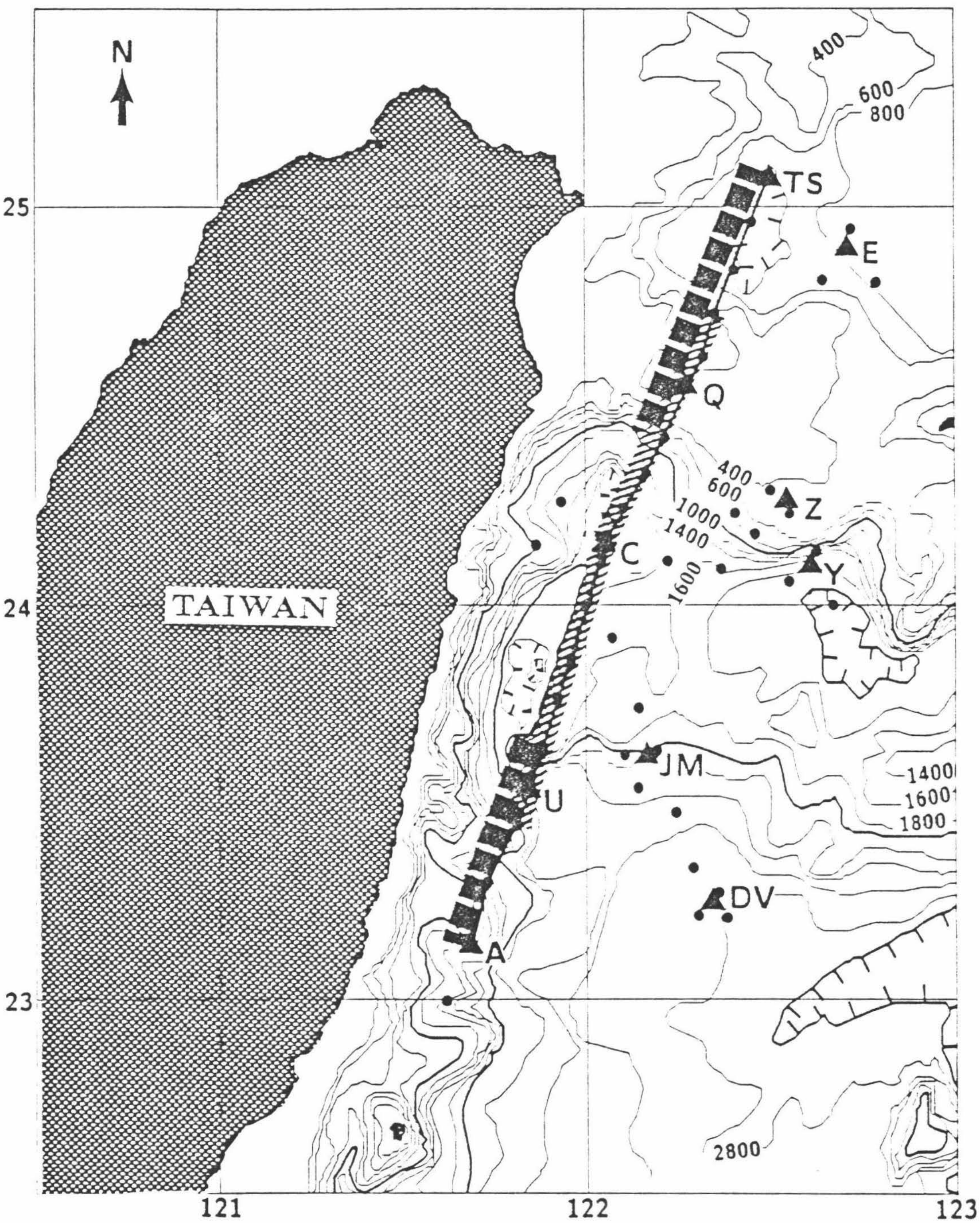
N
TAIWAN
25
24
23
121
122
123
400
600
800
TS
E
Q
400
600
1000
1400
1600
Z
C
Y
JM
U
1400
1600
1800
DV
A
2800

the source and receiver locations are determined (Sinton, 1982). The shotline records for each OBS were then demultiplexed and each of the sensor channels was plotted in record section format.

For each of the three OBSs studied, the signal-to-noise ratio was much better for the hydrophone than for either of the two geophones, therefore the hydrophone data were chosen for analysis (Figure 6). The poor quality of the geophone data is probably due to the fact that all of the instruments were deployed in an area of relatively thick (200-1000 m) sediments (Lu et al, 1977). This may have resulted in poor coupling between the geophones and the bottom causing sediment reverberation effects that show up as ringing on the geophone records. This occurred in spite of the fact that HIG OBSs are thought to be the best coupled instruments available (Sutton et al., 1977).

DATA ANALYSIS

The three OBS-shotline combinations chosen for analysis are shown in figure 5. The most southerly receiver, OBS A (at a depth of 2240 m), was located in an area of relatively smooth bottom. The central receiver, OBS C (at a depth of 3130 m), was located at the base of a major change in slope to the north. OBS TS (at a depth of 1300 m), the most northerly receiver, was located on the shelf of the East China Sea. Each shotline consists of closely spaced (200-500 m) airgun shots and a few widely spaced explosive shots. The airgun used in this experiment was a small one (60 in^3), consequently clear first arrivals can only be seen to a very limited range (about 20 km) in the record

Figure 6

Comparison between the hydrophone and the vertical geophone for OBS C. The geophone shows a poor signal-to-noise ratio that is probably caused by poor coupling with the bottom.

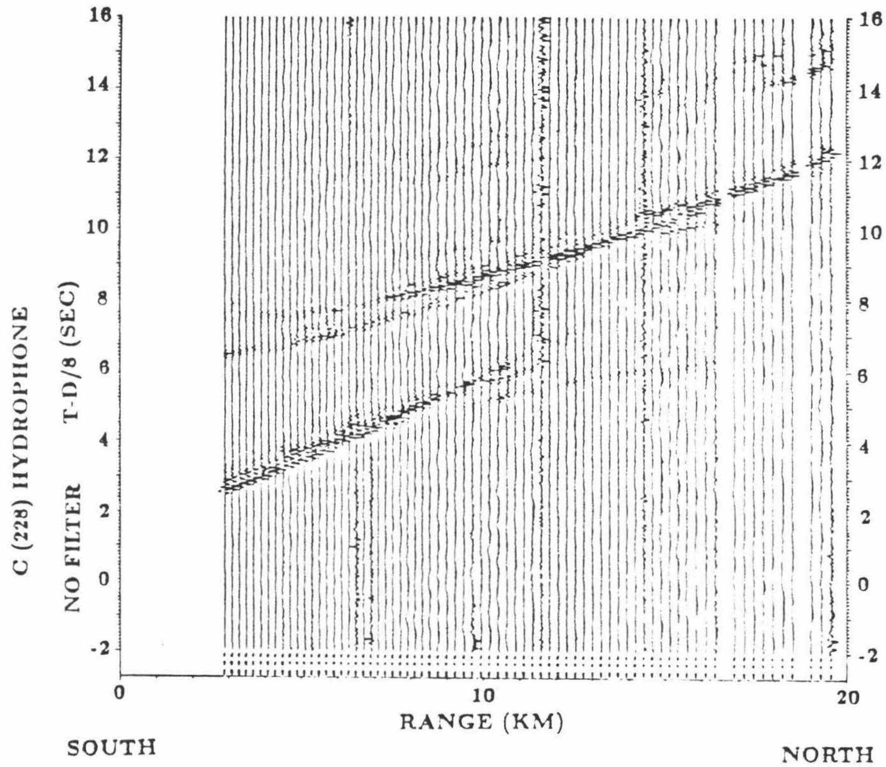

C (228) HYDROPHONE
NO FILTER T-D/8 (SEC)
RANGE (KM)
SOUTH
NORTH

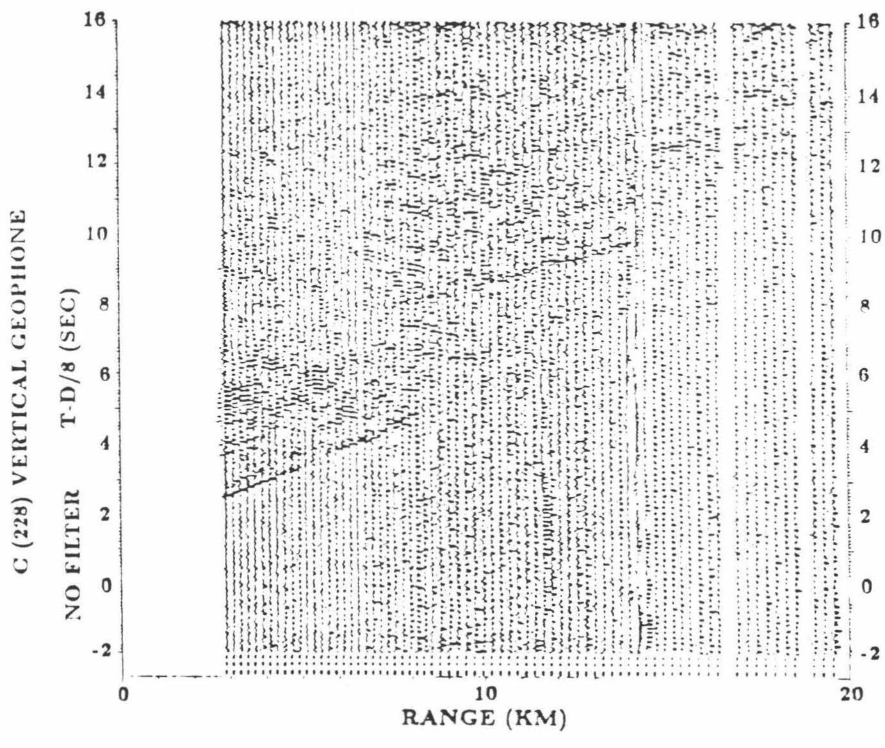

C (228) VERTICAL GEOPHONE
NO FILTER T-D/8 (SEC)
RANGE (KM)

sections. The larger explosive shots are used to extend the useful ranges of the profiles to more than 50 km in most cases.

The hydrophone record sections were plotted using a reducing velocity of 1.51 km/sec (average water column velocity). Water wave travel times were measured and the shot-to-receiver distances were corrected. The record sections were then filtered using a 6-pole Butterworth filter with a 4-14 Hz bandpass and replotted using a reducing velocity of 8.0 km/sec (Figures 7,8,9). Unfortunately, due to technical problems during the cruise, no bathymetric or reflection seismic data were collected along the shotlines. This severely limits the detail possible in the analysis and interpretation of the record sections since it was not possible to make any detailed topographic or sediment thickness corrections to the record sections. (Bathymetric corrections from published bathymetry were made in the raytrace modeling which will be discussed later.)

As a first approximation to the structure, the record sections were interpreted by fitting straight-line segments to the first arrivals. Initial velocity-depth models consisting of constant velocity layers were then calculated for each shotline. Shotlines A and TS are single-ended lines, and as such, no determination of layer dip is possible by the above method. Shotline C, however, is a split-spread line and shows a marked asymmetry between the two sides of the profile indicating that significant layer dip is to be expected.

The simple velocity-depth models obtained for each shotline were used as the basis for further analysis. A model was prepared that included the local bottom topography (based on published bathymetry

Figure 7

Record section for OBS A. The upper figure shows the arrivals that were modeled.

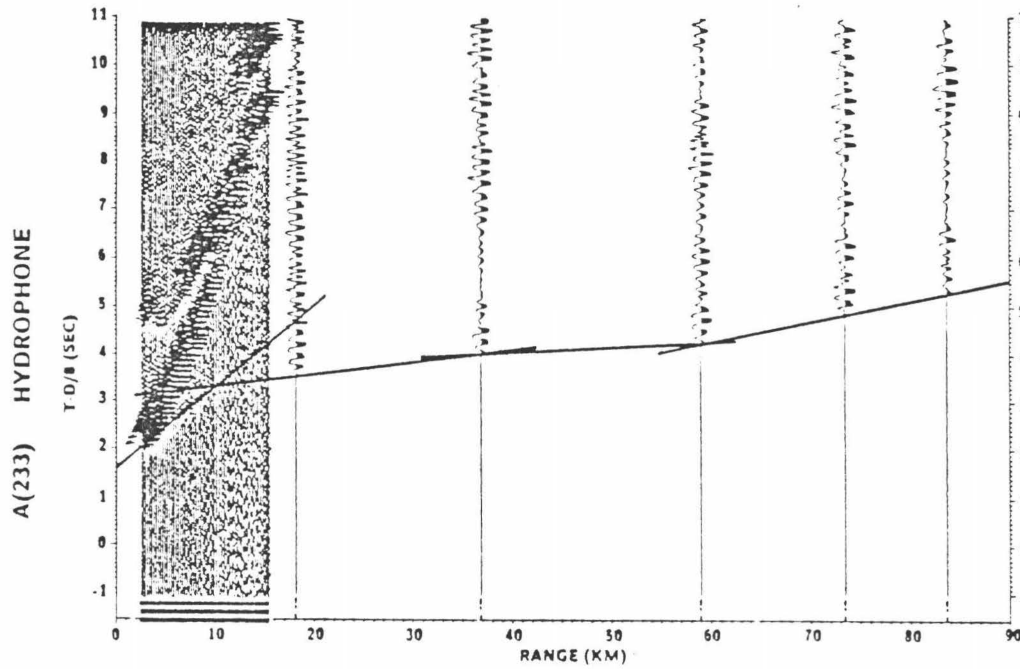
A(233) HYDROPHONE
T-D/8 (SEC)
RANGE (KM)

SOUTH

NORTH

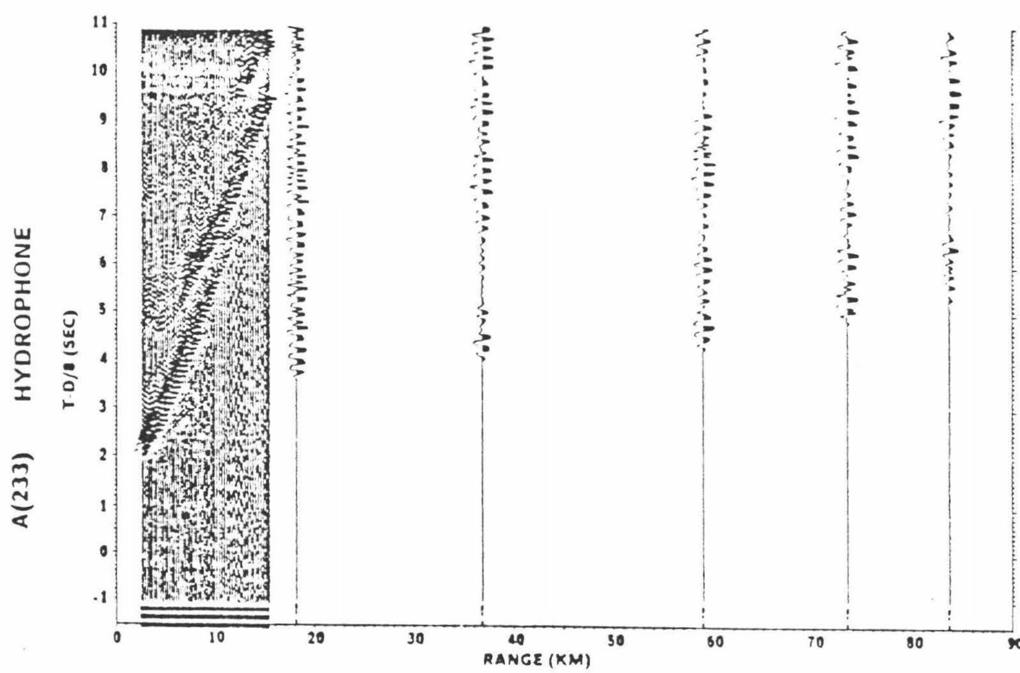
A(233) HYDROPHONE
T-D/8 (SEC)
RANGE (KM)

Figure 8

Record section for OBS C. The upper figure shows the arrivals that were modeled. The obvious asymmetry of the arrivals indicates that significant layer dip is present.

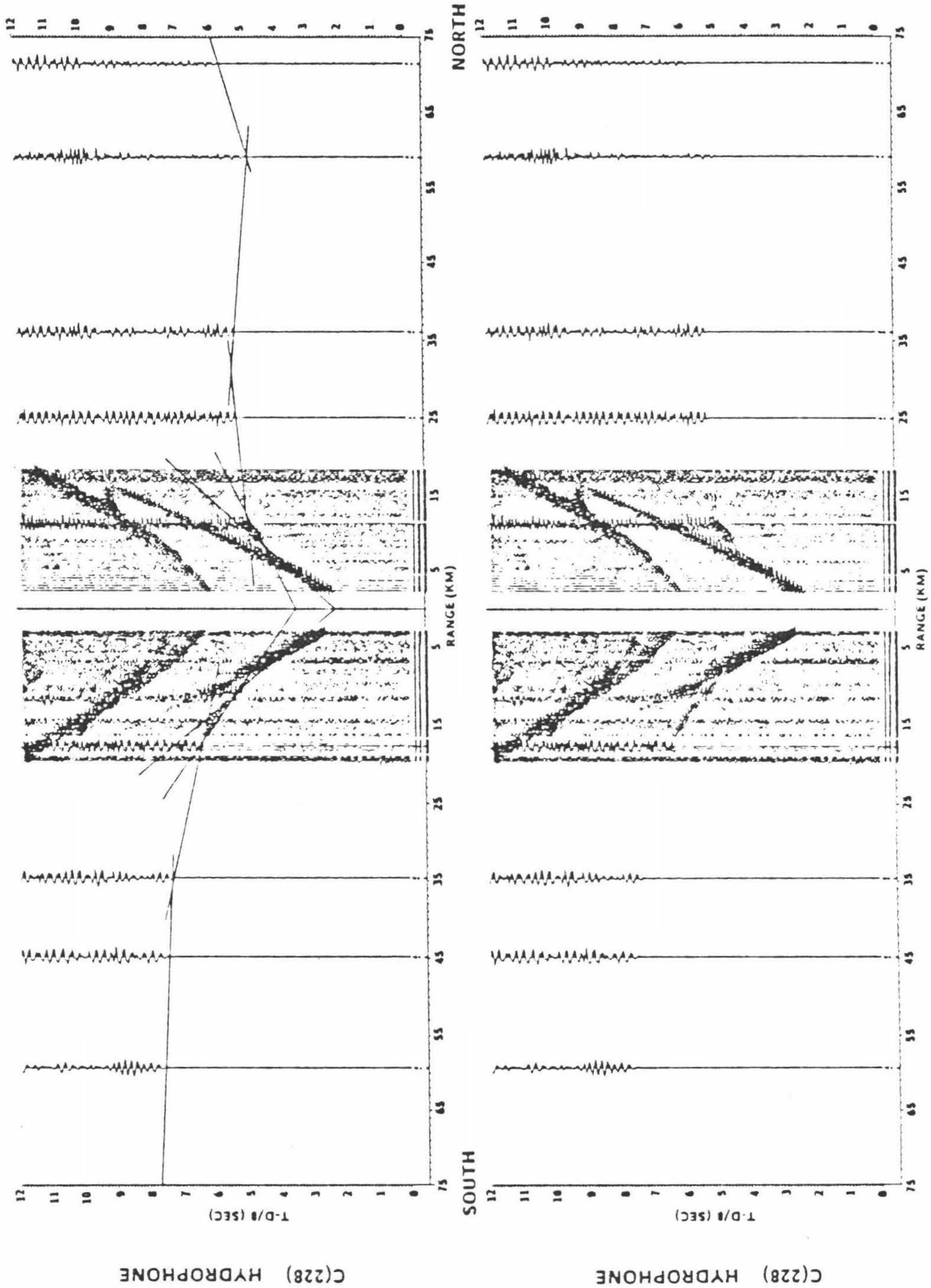
NORTH
SOUTH
RANGE (KM)
T-D/8 (SEC)
C(228) HYDROPHONE
C(228) HYDROPHONE

Figure 9

Record section for OBS TS. The upper figure shows the arrivals that were modeled.

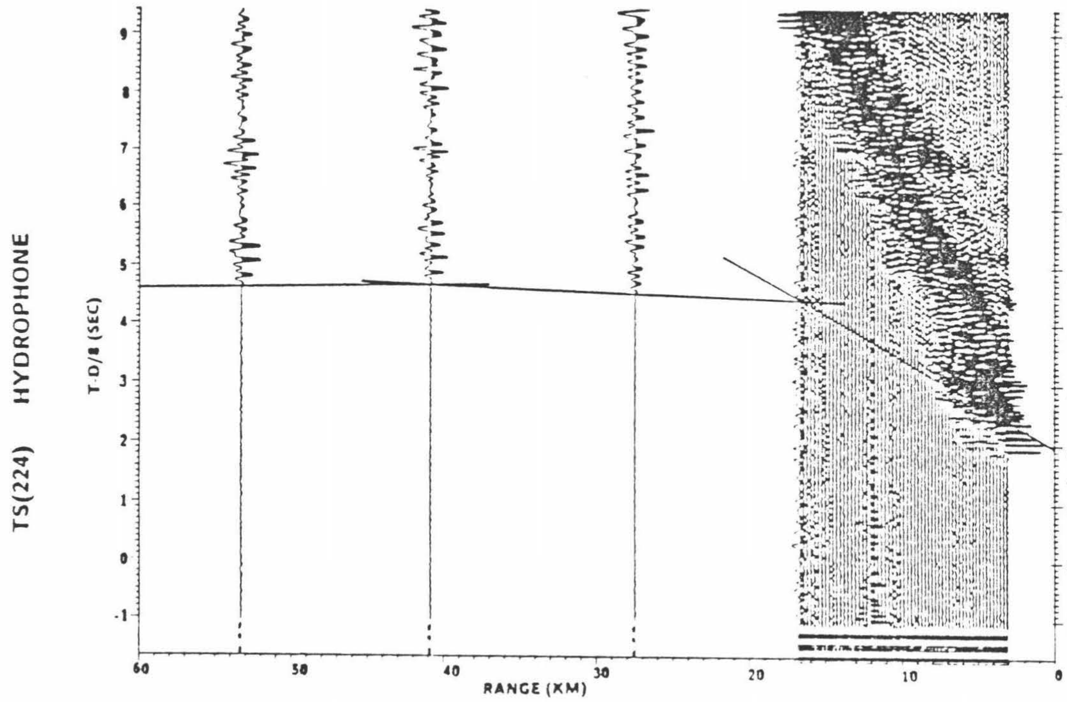
TS(224) HYDROPHONE
T-D/8 (SEC)
RANGE (KM)

SOUTH NORTH

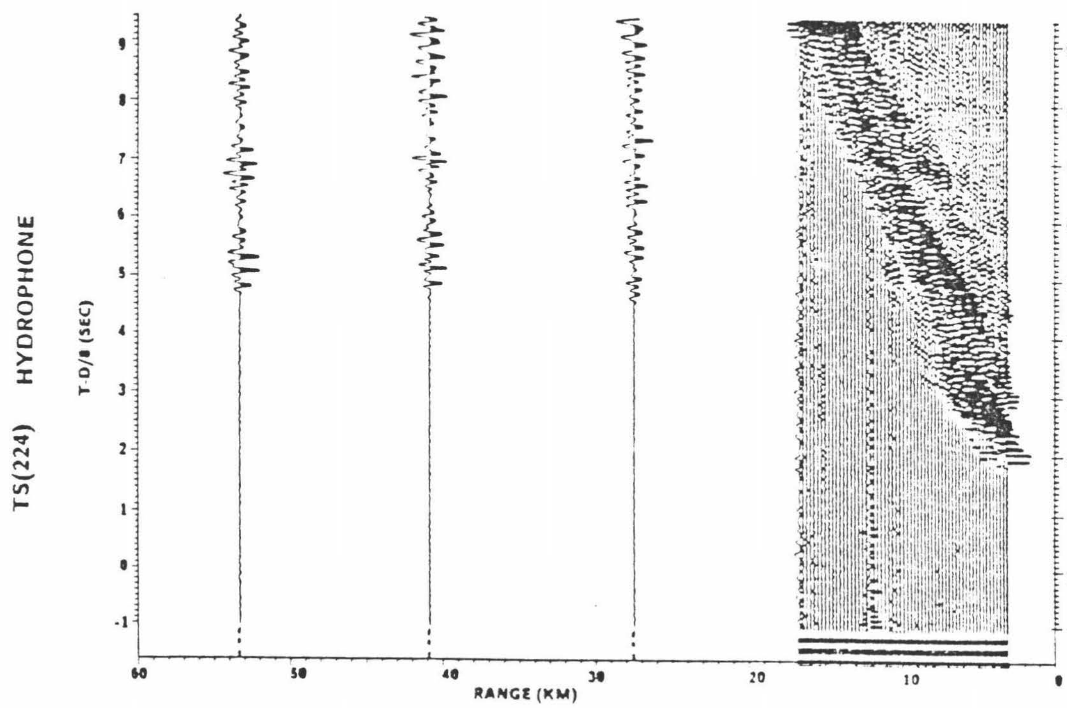
TS(224) HYDROPHONE
T-D/8 (SEC)
RANGE (KM)

(Menard and Chase, 1978)) and the average velocity-depth function from the line C data. A raytrace program written by Sinton (1982), using an algorithm of Gebrande (1976), was used to propagate rays through the models. By incorporating the sea bottom relief in the models we effectively include large scale topographic corrections in the analysis.

The initial model consisted of horizontal, constant velocity layers (Figure 10). A slight vertical velocity gradient was introduced into each layer in the model to produce refracted rays in the raytrace. This model was then perturbed through several generations. The travel-time data from each model were matched to the hydrophone data through a trial-and-error process in which the short range data (shallow layers) were matched first and the farthest range data (deepest layers) were matched last. During the course of this modeling it was determined that a low velocity sediment layer, not evident on the record sections as a first arrival, would have to be included in the model in order to fit the arrivals for the shallowest crustal layer. The velocity for this sediment layer was chosen to be 2.0 km/sec based on the sonobuoy work of Leyden (1973). The resulting thickness of this layer, as determined by modeling for each shotline, agrees quite well with the sediment isopach map of Lu (1977).

RESULTS

The final velocity-depth model obtained in this study is shown in figure 11. As expected, significant layer dip was required in the

Figure 10

The initial model used in the raytracing. The general bathymetry is included at the top of the model. OBS locations are shown by the triangles. A sample raytrace is shown for OBS A. (V.E. = 6.25 X)

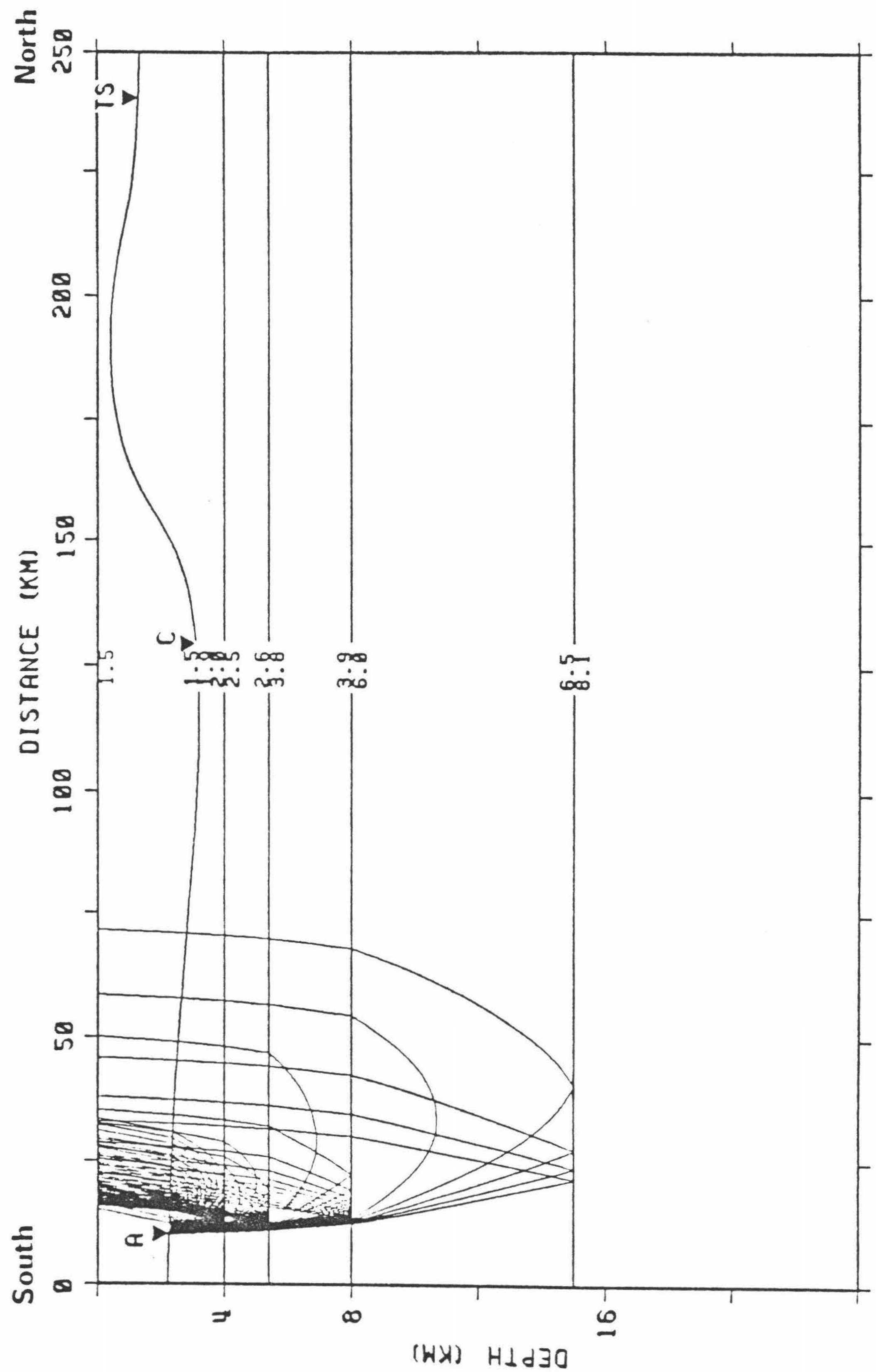

North
South
DISTANCE (KM)
DEPTH (KM)
0
50
100
150
200
250
4
8
16
TS
C
A
1.5
2.6
3.8
3.9
6.0
6.5
8.1

Figure 11

The final velocity-depth model obtained by the raytrace modeling. The model is characterized by an area of downwarping and crustal thickening to the south of OBS C. The patterned region shows the areas in the model that are constrained by the raytraces. (V.E. = 5 X)

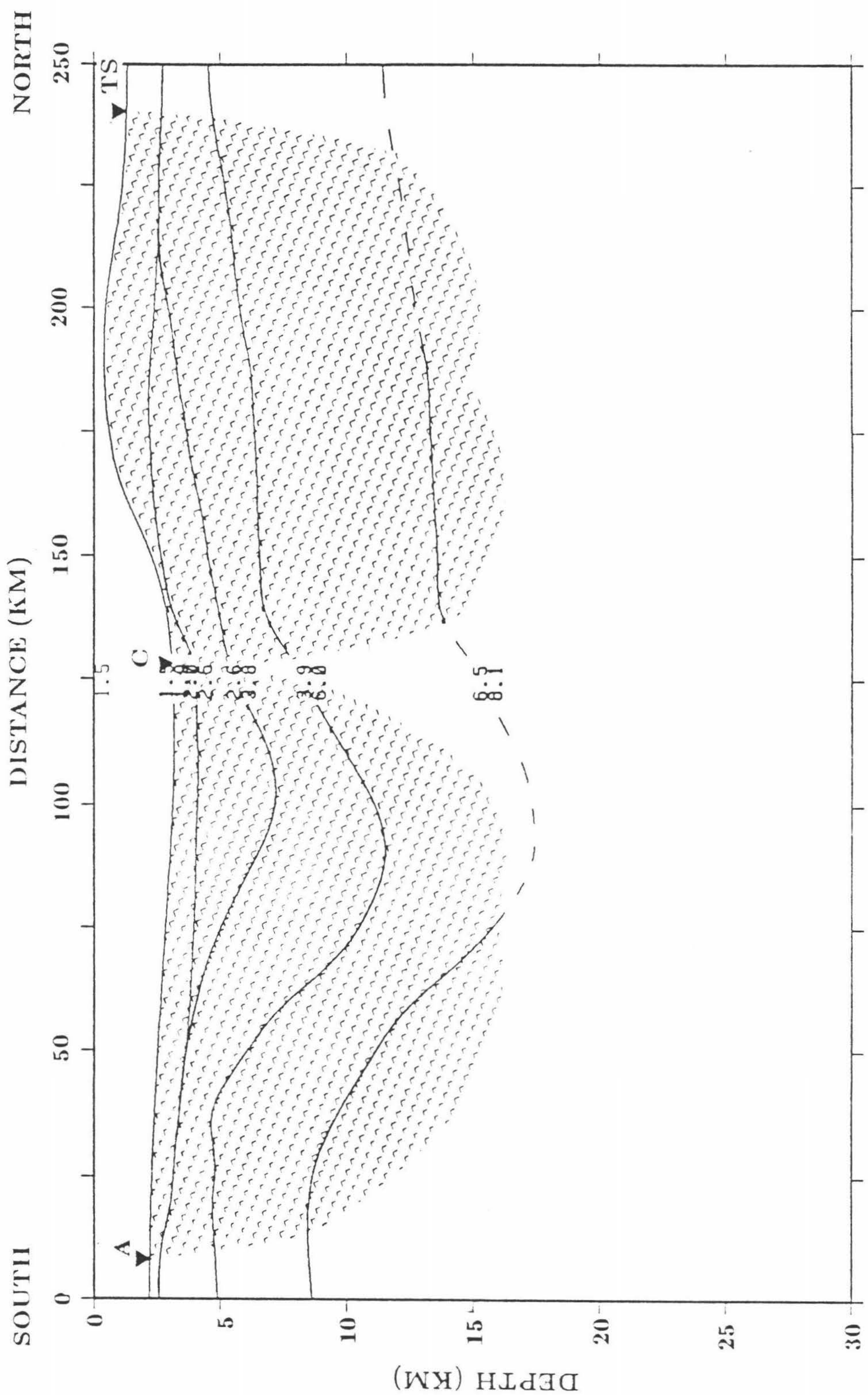
SOUTH
NORTH
DISTANCE (KM)
DEPTH (KM)
0
50
100
150
200
250
0
5
10
15
20
25
30
A
C
TS
1.5
6.5
8.1

final model to properly match the travel-time data of the record sections. The final model consists of the following layers:

1.) The shallowest layer is a sediment layer with a velocity (assumed) of 2.0 km/sec. The thickness of this layer varies from 1.5 km at the north end of the model (on the continental shelf), to 0.2 km in the deep water at the south end of the line. The thinning of this layer is probably a result of increasing distance from the sediment source area.

2.) The second layer in the model was not seen in the OBS A or OBS TS data and was therefore modelled as a wedge of material which pinches out both to the north and south of OBS C. This layer has a velocity of 2.55 km/sec and a maximum thickness of 3 km. It may represent a layer of sediments derived from the rapid uplift of nearby Taiwan or sediments accreted by subduction along the Ryukyu Trench.

3.) The third layer consists of material with a velocity of 3.85 km/sec and has an average thickness of 2.0 - 2.5 km. This layer probably represents the pillow basalts of the upper oceanic crust itself and has a velocity consistent with oceanic layer 2A (Houtz and Ewing, 1976; Clague and Straley, 1977; Christensen and Salisbury, 1975).

4.) The fourth layer in the model is composed of a thick (6 - 7 km) layer with a velocity gradient of 6.0 - 6.5 km/sec. This velocity is at the high end of the range usually attributed to oceanic layer 2B and is at the same time lower than expected for layer 3 (Clague and Straley, 1977).

The fourth layer in the model exhibits the effects of the decrease in resolution with depth for these data. The energy returned from this layer falls in the range where the airgun arrivals die out and we are forced to rely on the sparse explosive shots. As a result, the model may not be a good representation of the actual velocity structure at these depths and this layer may represent an averaging or "blending" of the actual velocity structure. Further evidence of the poor resolution at this depth is the fact that arrivals from material with a mantle velocity (8.1 km/sec) can only be seen on the northern half of the OBS C record section.

Because this model was based on the velocities obtained from the central receiver, OBS C, there are some problems in the modeling of the other OBSs. Figures 12,13,and 14 show the comparisons of the travel-time data from the raytrace model with the actual record sections.

The travel-time data matches the OBS C record section to within 0.1 second in most places, with the exception of the northernmost explosive shot (Figure 12). The travel-time plot is in good agreement with the OBS A data out to about 30 km (Figure 13). Beyond this point the raytrace arrivals are consistently late. A better match to arrivals beyond 30 km might be possible with further perturbations to

Figure 12

Comparison of the travel-time plot of the raytrace with the actual record section for OBS C. The travel-time data match the record section arrivals to within 0.1 sec except for the northernmost shot.

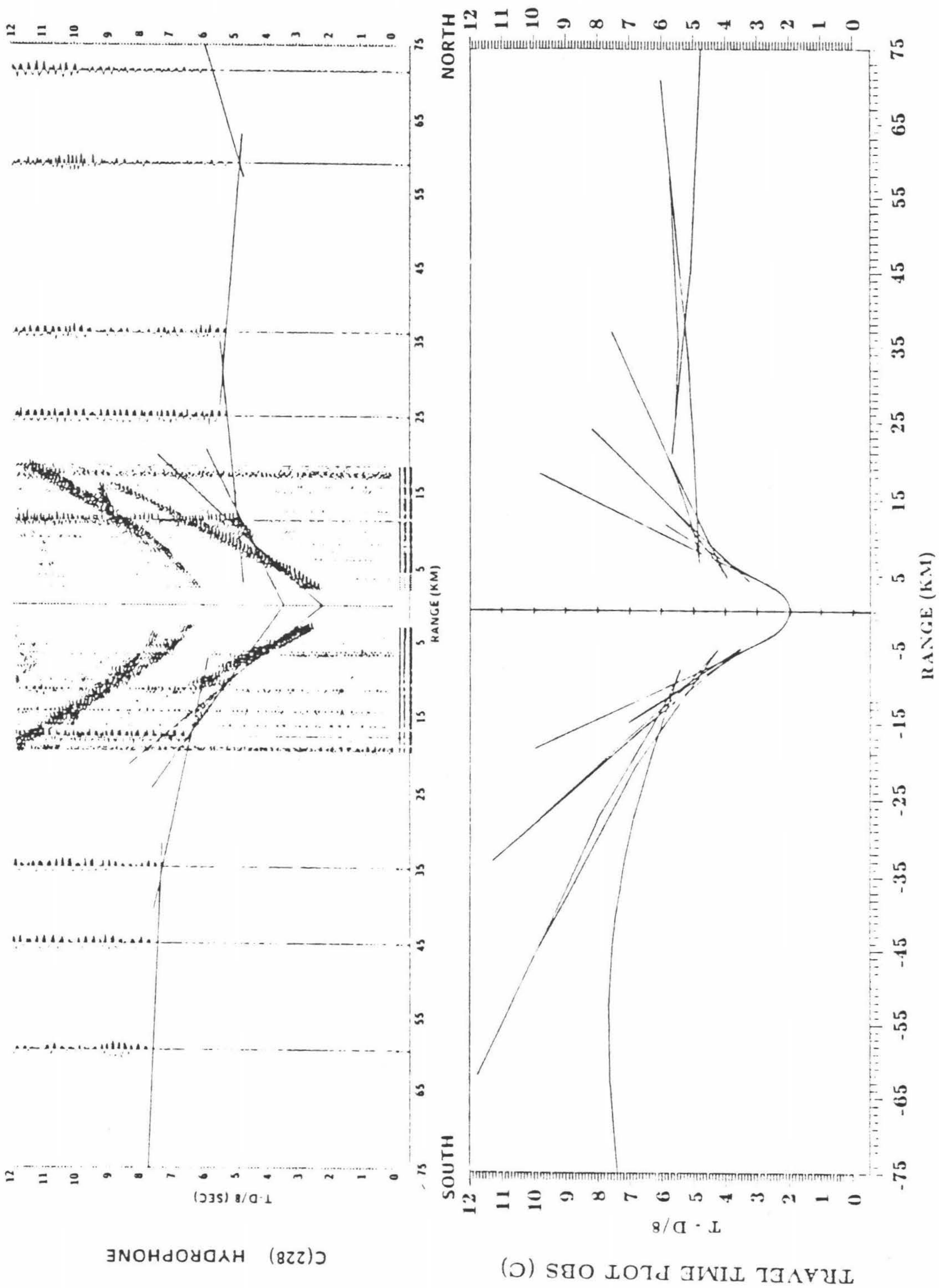
C(228) HYDROPHONE
T-D/8 (SEC)
RANGE (KM)
NORTH
SOUTH
T - D/8
RANGE (KM)
TRAVEL TIME PLOT OBS (C)

Figure 13

Comparison of the travel-time plot from the raytrace with the actual record section for OBS A. The travel-time plot is in good agreement with the data out to about 30 km.

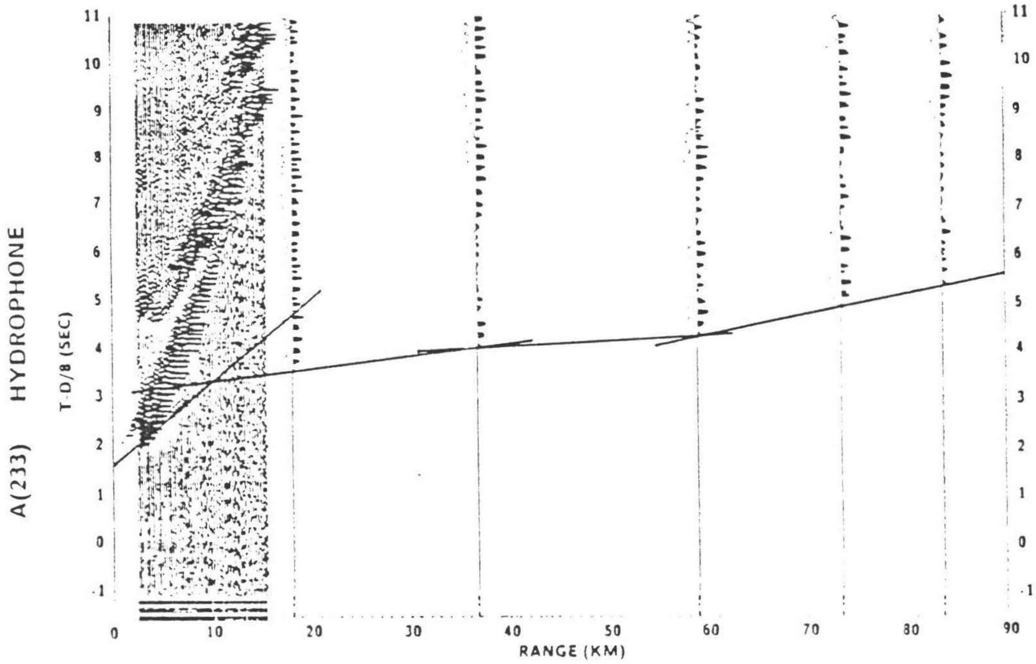
A(233) HYDROPHONE
T-D/8 (SEC)
RANGE (KM)
0
10
20
30
40
50
60
70
80
90

SOUTH NORTH

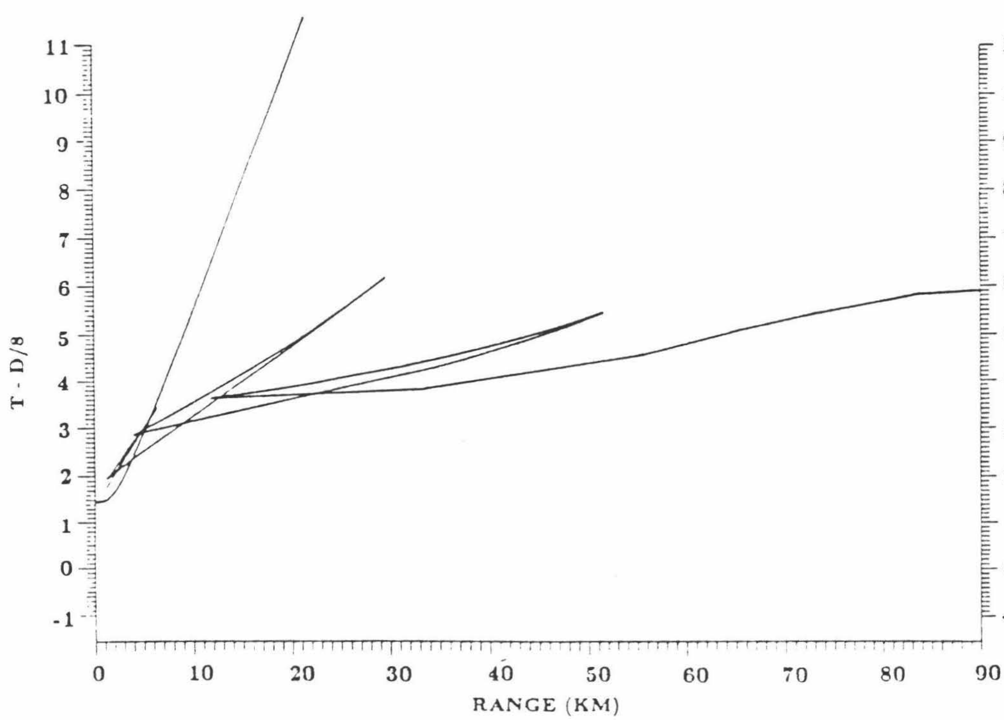
T - D/8
RANGE (KM)
0
10
20
30
40
50
60
70
80
90

Figure 14

Comparison of the travel-time plot for the raytrace with the actual record section of OBS TS. The travel-time plot matches the data for this OBS quite poorly.

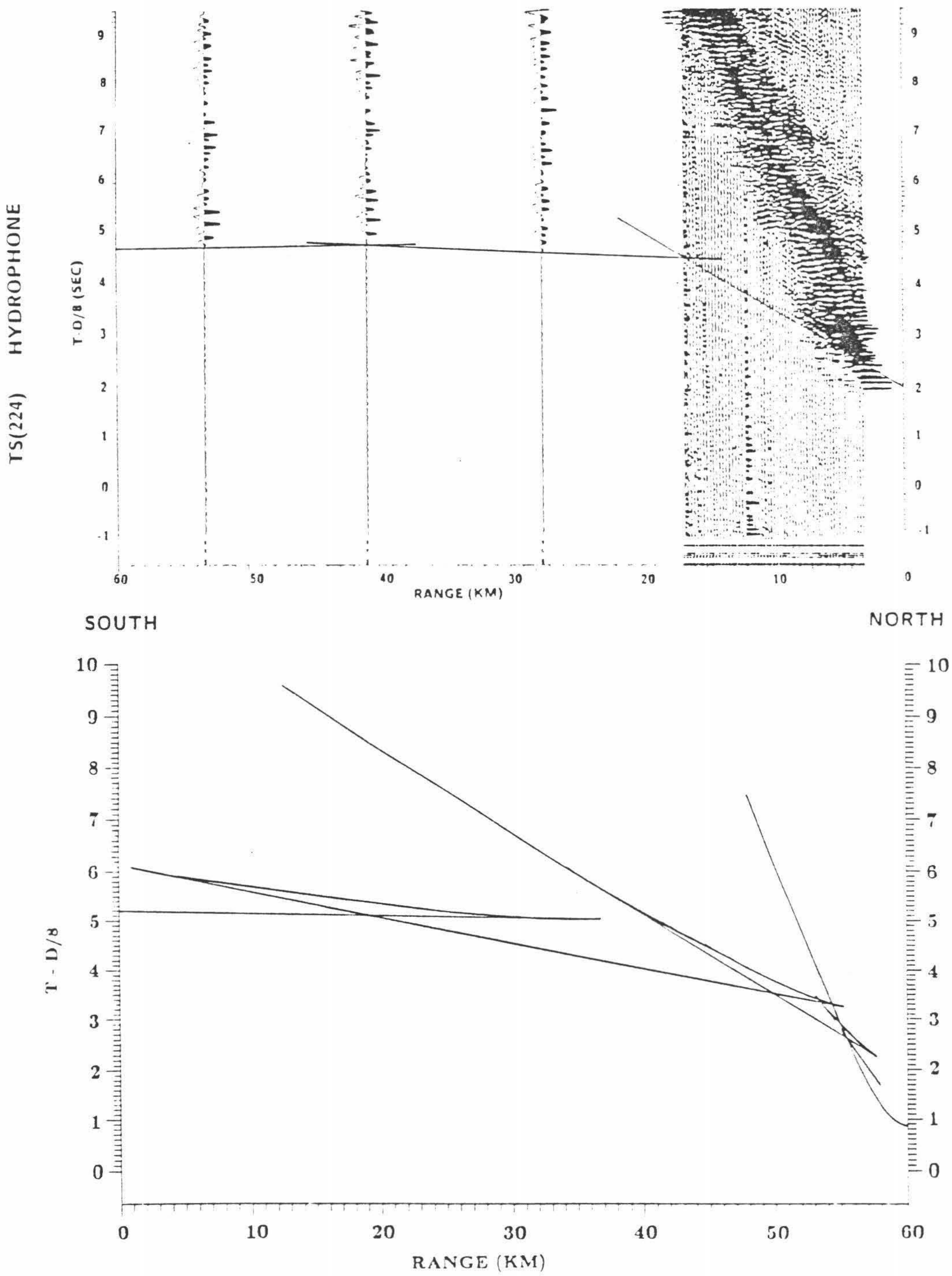
TS(224) HYDROPHONE
T-D/8 (SEC)
RANGE (KM)
SOUTH
NORTH
T - D/8
RANGE (KM)

the model and/or an increase in the velocity of the 6.0 - 6.5 km/sec layer. However, we believe that the quality of the data does not merit further modeling.

For the same reasons, no further modeling was attempted for the OBS TS data, even though the model matches the data very poorly (Figure 14). OBS TS is located on the shelf of the East China Sea. The poor match of the model with the data is probably the result of lateral changes in velocity and crustal thickness associated with the transition from oceanic-type, through arc-type, to continental-type crustal material. In fact, the data indicates that a better match could be obtained by increasing the depth and velocity of the 6.0 - 6.5 km/sec layer in the model.

As the discussion above indicates, the model is not well constrained beneath OBS A or OBS TS. The structure beneath those receivers should therefore be considered with caution. The model is much better constrained in the vicinity of OBS C. There is however, a certain amount of ambiguity present in the model since slightly different velocities, combined with different layer dips and depths, could also be made to fit the arrivals. These possible errors are cumulative with depth in the model. We estimate that the velocity errors in the model range from 0.05 km/sec at the top of the model to 0.30 km/sec for the deepest interface. Such variability could lead to depth errors on the order of from 0.07 km for the shallow layers to 0.75 km at depth. Although the absolute accuracy of the velocities and depths in the final model are questionable, the overall structure shown in the model is necessary to adequately match the first arrivals.

DISCUSSION

Wu (1970, 1978) concluded that the Ryukyu arc is displaced to the north about 100-120 km east of Taiwan by a right-lateral trench-to-trench transform fault (Figure 1). This transform was defined by a few right-lateral, strike-slip focal mechanisms that appeared to define a northerly striking fault plane near 123° E. The northerly offset segment of the subduction zone was then thought to connect to the plate boundary in Taiwan (the Longitudinal Valley) near 24° N. This offset of the Ryukyu arc has been generally accepted (Chai, 1972; Karig, 1973; Juan, 1975; Seno and Kurita, 1978; Lin and Tsai, 1981, Juan et al., 1983), probably because of the overall lack of data from the area.

The Ryukyu Trench, which is well defined along the northeastern part of the arc, becomes broader and shallower as it approaches Taiwan and cannot be easily defined west of 123° E. This may be a result of the more oblique angle of subduction in this area as well as the increased sedimentation from Taiwan. It is also unlikely to be a coincidence that this is also the area where a submarine ridge, the Gagua Ridge, enters the trench from the south. Although Bowin et al.(1978) state that the Gagua Ridge is an extinct spreading center, Mrozowski et al.(1982) believe that the Gagua Ridge is an upfaulted sliver of oceanic crust, perhaps similar to the ridges found bordering fracture zones.

Regardless of its origin, the collision of the Gagua Ridge with the Ryukyu Trench appears to be having a significant effect on the nature of subduction in this area. It is possible that the right-lateral strike-slip focal mechanisms used by Wu (1970, 1978) to define the offset of the trench are in some way related to the collision of the Gagua Ridge with the inner slope of the Ryukyu Trench near 123^{o}E.

The free-air gravity map of Bowin et al. (1978) shows no apparent offset of the arc and seems to indicate that the trench extends up to the continental margin of eastern Taiwan. Ho (1986) cites this gravity data, as well as personal communications with French scientists, as evidence that the Ryukyu Trench may extend directly to the east coast of Taiwan. This hypothesis of a continuous trench is supported by Suppe (1981, 1984) who developed a simple plate-tectonic kinematic model for the arc-continent collision near Taiwan. He determined that a continuous Ryukyu Trench was necessary if the back-arc spreading of the Okinawa Trough was to be accounted for by his model.

Very little seismic refraction work has been done in the area near Taiwan. However, a few refraction studies have been conducted to the north and east in the Okinawa Trough, the Ryukyu arc, and the western Philippine Sea (Figure 15). Several two-ship seismic refraction profiles were recorded in various regions of the Philippine Sea by Murauchi et al. (1968). They found that the Philippine Sea basin near Taiwan has a fairly ´normal´ oceanic crustal structure except that layer 2 has a slightly lower average velocity and is slightly thinner than the Pacific average. Layer 3 was also found to be thinner than normal. The crustal structure of one of their profiles across the Ryukyu arc is shown in Figure 16. This profile shows a downwarping of the layers on the landward side of the trench axis.

Figure 15

Map of the area between Taiwan and Kyushu showing the locations of other refraction profiles across the Ryukyu Arc. From north to south:

Ludwig (1973) - (fine hachure)

Murauchi (1968) - (stipple)

Leyden (1973) - (block)

This study - (coarse hachure)

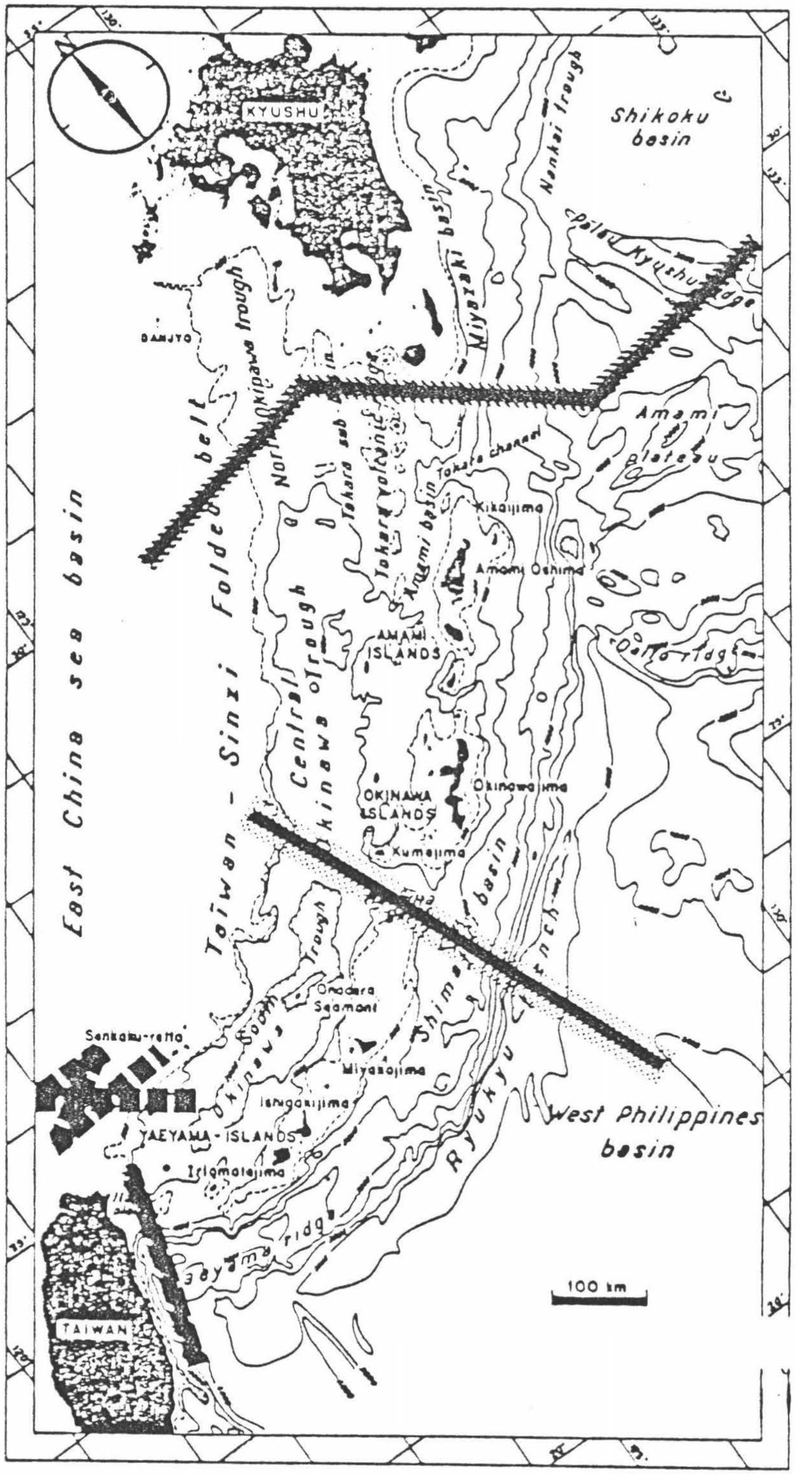
KYUSHU
Shikoku basin
Nankai trough
Miyazaki basin
Amami Plateau
Tokara channel
Kikaijima
Amami Oshima
AMAMI ISLANDS
OKINAWA ISLANDS
Okinawajima
Kumejima
East China sea basin
Taiwan - Sinzi Folded belt
Central Okinawa trough
Tokara volcanic
Amami basin
DANJYO
Senkaku-retto
Onodera Seamont
Miyakojima
Ishigakijima
YAEYAMA-ISLANDS
Iriomotejima
West Philippines basin
TAIWAN
100 km

Figure 16

Structure section of Murauchi et al. (1968) running northwest-southeast from the continental shelf of the East China Sea into the West Philippine Basin.

MURAUCHI ET AL. (1968)

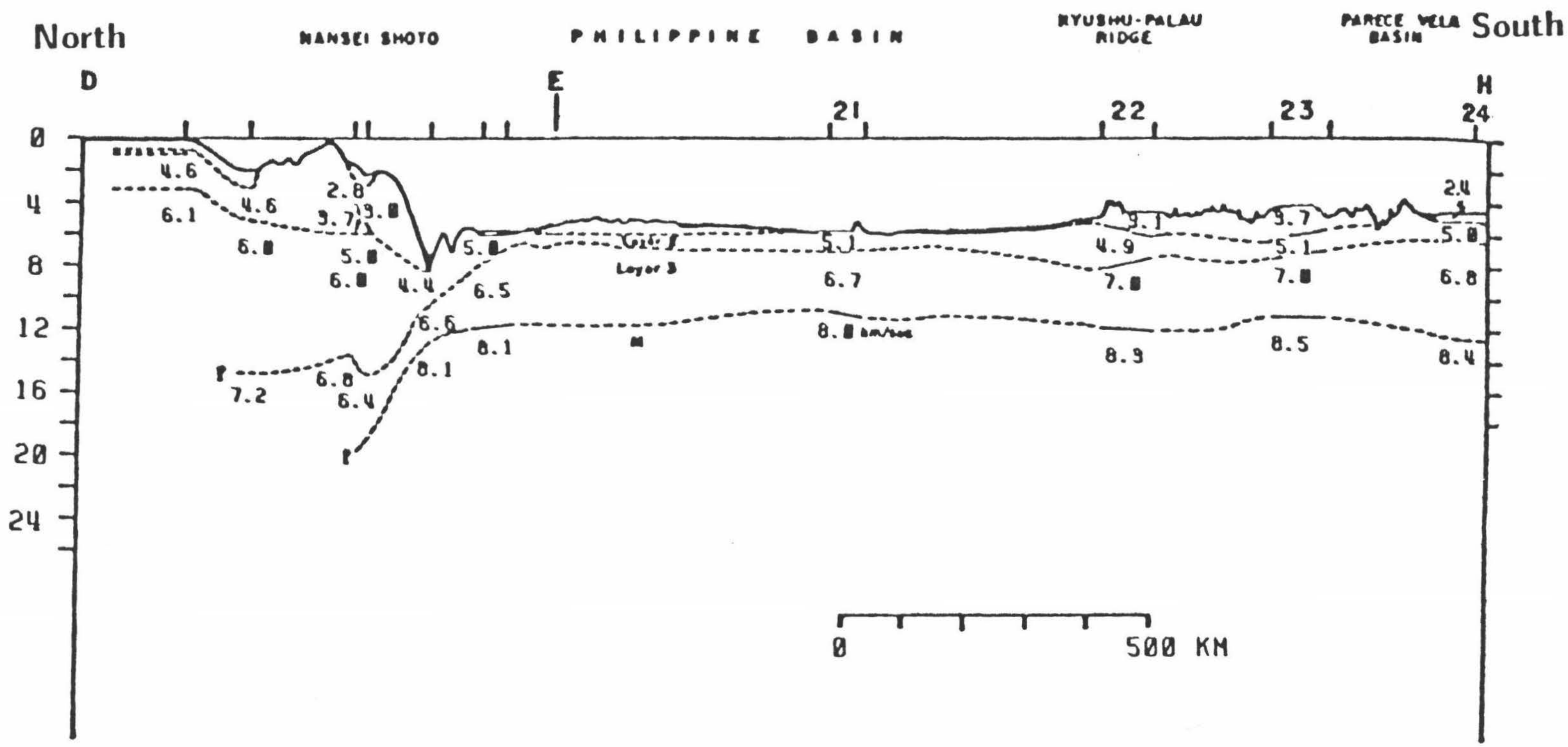

Structure section northwest–southeast from the continental shelf of the Eastern China Sea into the Parece Vela basin.

Ludwig et al.(1973) conducted several two-ship refraction lines across the Ryukyu arc off the Southern end of Kyushu. They found that the crust seaward of the trench is oceanic, but with a thinner layer 3. The trench slope was found to be underlain by an accumulation of sediment that fills a crustal trough believed to represent a filled portion of the Ryukyu Trench (Figure 17).

Leyden et al. (1973) used sonobuoy refraction measurements in the East China Sea to determine the velocities and thicknesses of the sediment cover and shallow basement which were then correlated with units encountered in drill holes on Taiwan (Figure 18). The velocities of these shallow layers agree quite well with the values found in our analysis.

There is a close similarity between the crustal velocity structure determined in our study and the above mentioned profiles across the arc to the northeast. Our profile exhibits nearly the same crustal velocities and thicknesses found in the above profiles. Our profile also shows the down-warping and crustal thickening typical of the trench area to the northeast. We believe that this data provide further evidence for the continuous nature of the Ryukyu arc in this area. Figure 19 shows the location we would pick for the trench based on our profile. The trench axis is chosen to be immediately seaward of the thickened low-velocity layers on the profile. This is in agreement with the trench location on the profiles to the north and east where the trench is well defined.

Figure 20 shows hypocenters ($M_b > 4.8$) located by the WWSN network during the period (1964-1982) projected onto a plane parallel to the

Figure 17

Structure section of Ludwig et al. (1973) extending west to east across the Ryukyu arc near Kyushu.

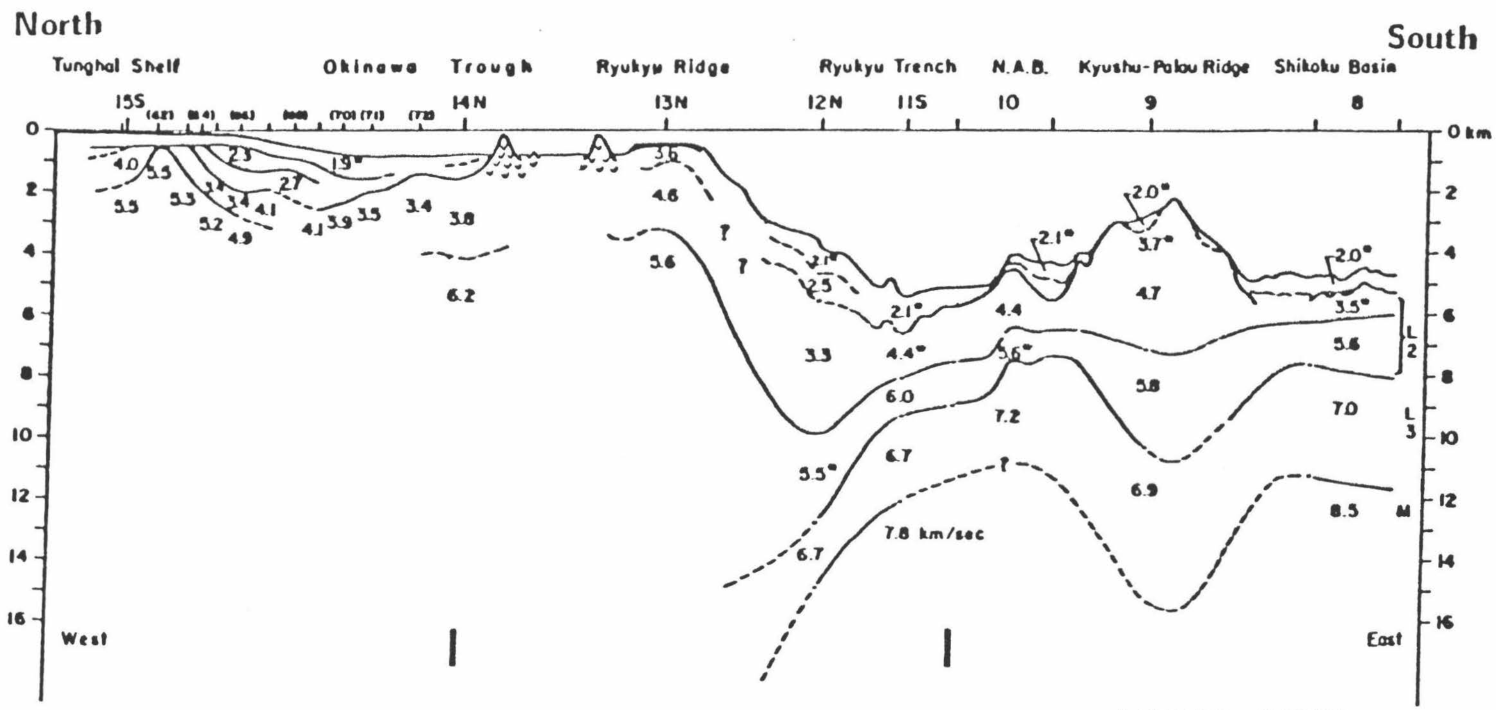
North
South
Tunghai Shelf
Okinawa Trough
Ryukyu Ridge
Ryukyu Trench
N.A.B.
Kyushu-Palau Ridge
Shikoku Basin
15S
14N
13N
12N
11S
10
9
8
0 km
7.8 km/sec
West
East

LUDWIG (1973)

Figure 18

Sonobuoy refraction results of Leyden et al. (1973) from the East China Sea north of Taiwan.

R. Leyden, M. Ewing, and S. Murauchi (1973)

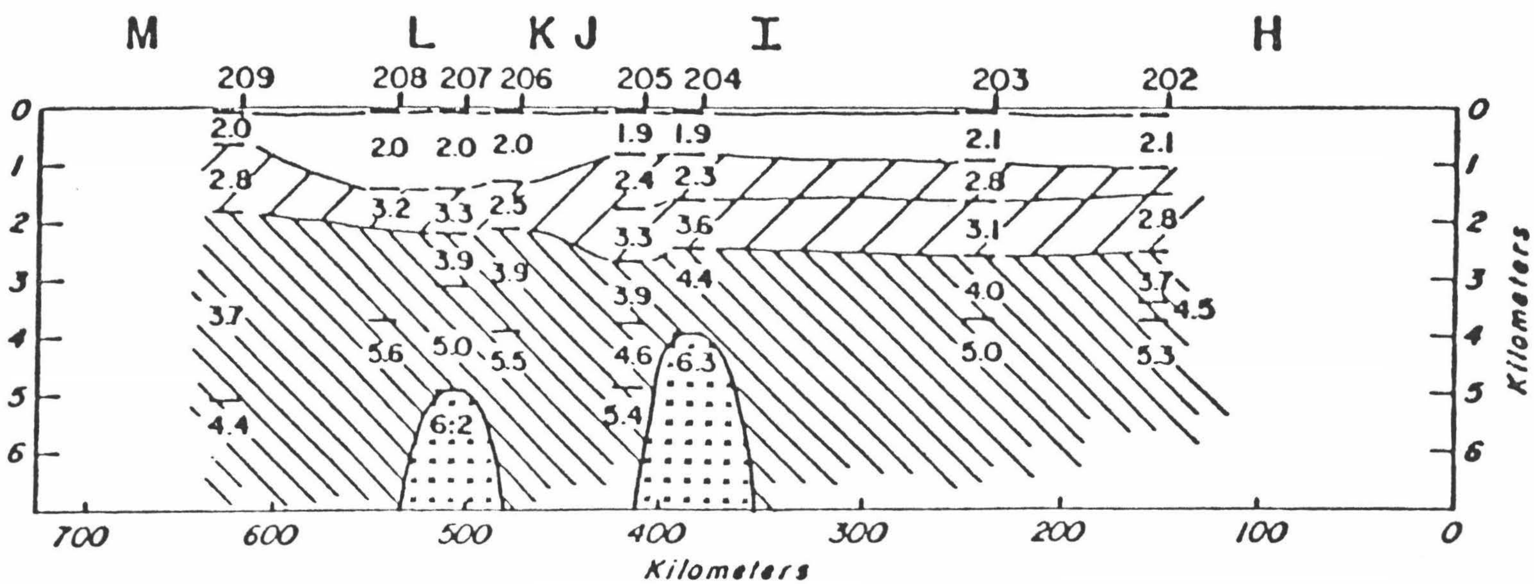

Figure 19

Map showing the location we would pick for the Ryukyu trench based on the results of this study (block pattern), and the northward offset of the trench (fine hachure) favored by Wu (1970, 1978).
Contour interval = 200 fathoms.

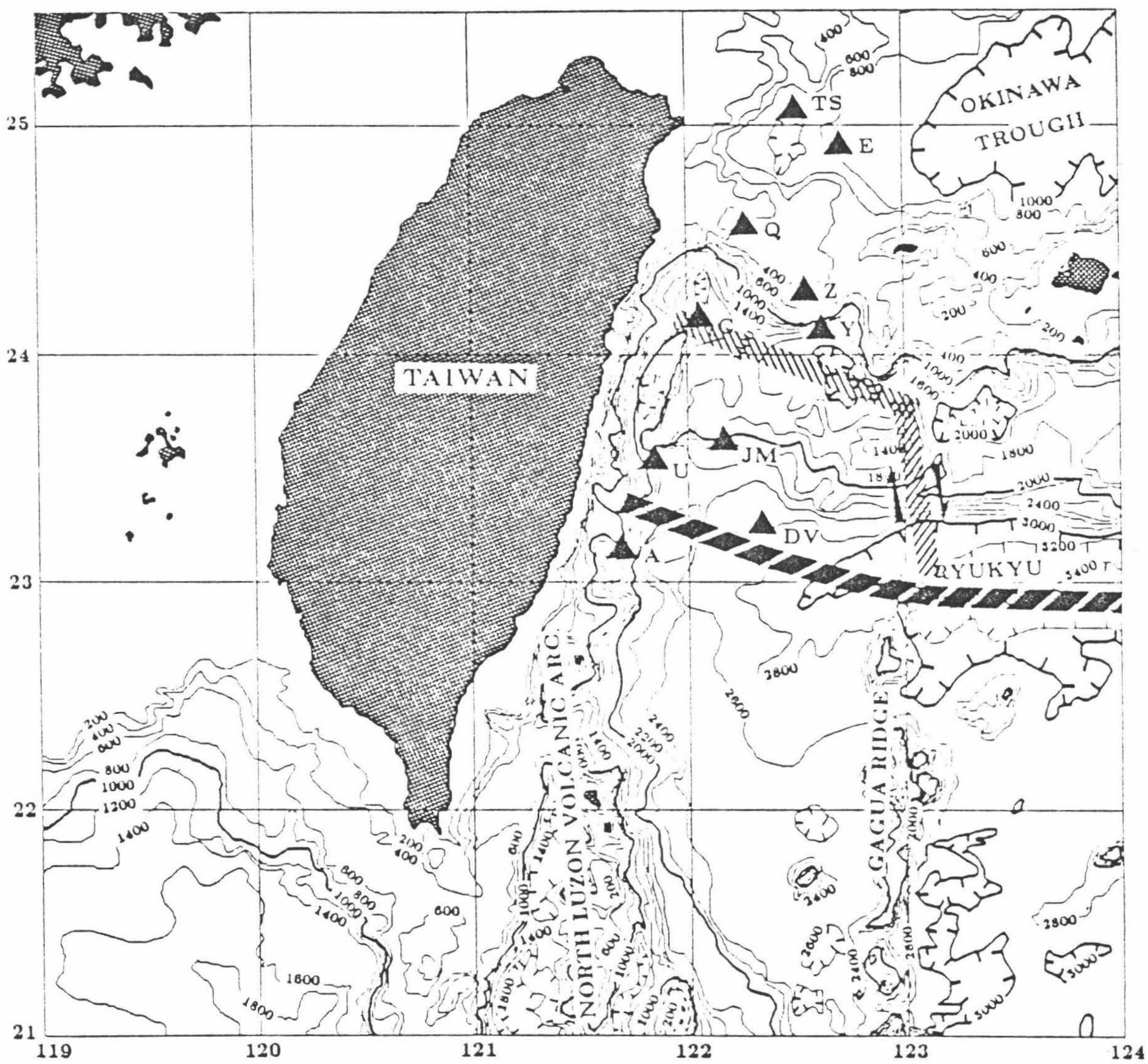
TAIWAN
OKINAWA
TROUGH
TS
E
Q
Z
Y
G
JM
U
DV
A
RYUKYU
NORTH LUZON VOLCANIC ARC
GAGUA RIDGE
25
24
23
22
21
119
120
121
122
123
124

line of our refraction profile. The crustal velocity structure and trench axis location of our study are shown along with the trench axis of Wu (1970, 1978). The hypocenter locations appear to define a subducting slab which is in better agreement with our trench axis location than with the more northerly position. All of the large events shown (and many of the intermediate ones) were found to have thrust-type focal mechanisms with moderate strike-slip components. One problem with any interpretation using hypocenters from WWSN is that the WWSN depths for shallow earthquakes are often too deep. Also, there is some ambiguity involved in defining the top of a subducting slab, since most of the larger events are internal to the slab.

Hypocenters (with $M_b > 2.0$) located by the Taiwan Telemetered Seismic Network (TTSN), during the period (1974-1976), were projected onto a plane nearly coincident with the line of our refraction profile by Tsai et al.(1978). Figure 21 shows this profile along with the trench locations of Wu (1970, 1978) and of this study. This profile seems to indicate that the northerly trench position of Wu (1970, 1978) is more consistent with the seismicity. However, the hypocenters located by TTSN may be significantly in error because of the poor azimuthal coverage for events in this area. The profile also includes a large number of shallow events from the eastern part of Taiwan that may be unrelated to subduction.

Figure 20

Hypocenters located by the WWSN network during the period (1964-1982) projected onto a plane parallel to the line of our refraction profile. The velocity structure of this study is shown at the top of the profile. The solid triangle shows the trench location of Wu (1970,1978) and the open triangle shows the trench location based on our crustal velocity model. The epicenters shown come from an area measuring 250 km north-south and 80 km east-west, parallel to our line, but centered 20 km to the east to avoid contamination with hypocenters from the island.

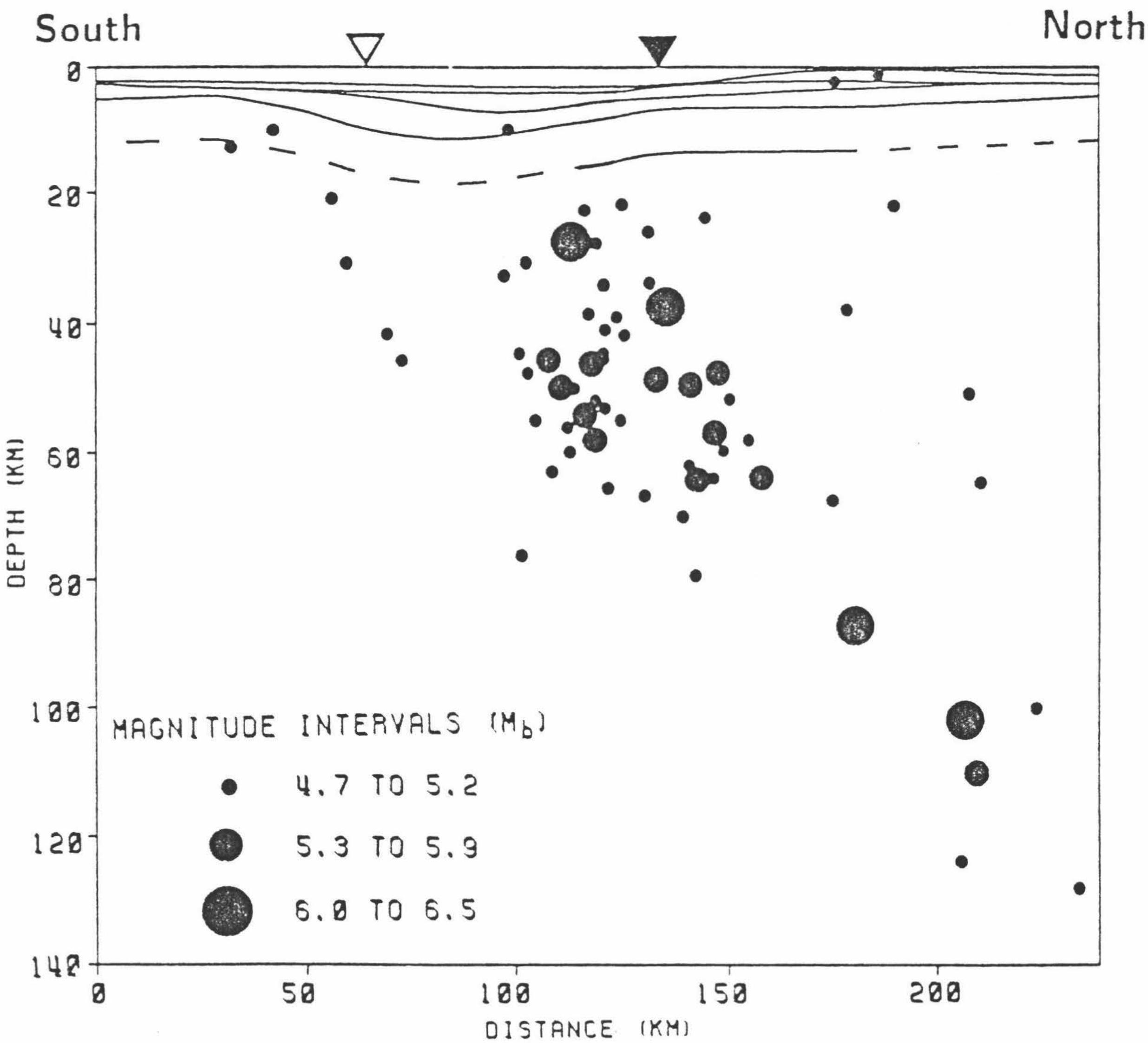
South
North
0
20
40
60
80
100
120
140
DEPTH (KM)
0
50
100
150
200
DISTANCE (KM)
MAGNITUDE INTERVALS (M_b)
4.7 TO 5.2
5.3 TO 5.9
6.0 TO 6.5

Figure 21

Hypocenters located by TTSN during the period (1974-1976) projected onto a plane parallel to our refraction profile (Tsai et al., 1978). The arrow at 24° N marks the trench location of Wu (1970, 1978) while the trench location based on our refraction results is marked by an open triangle.

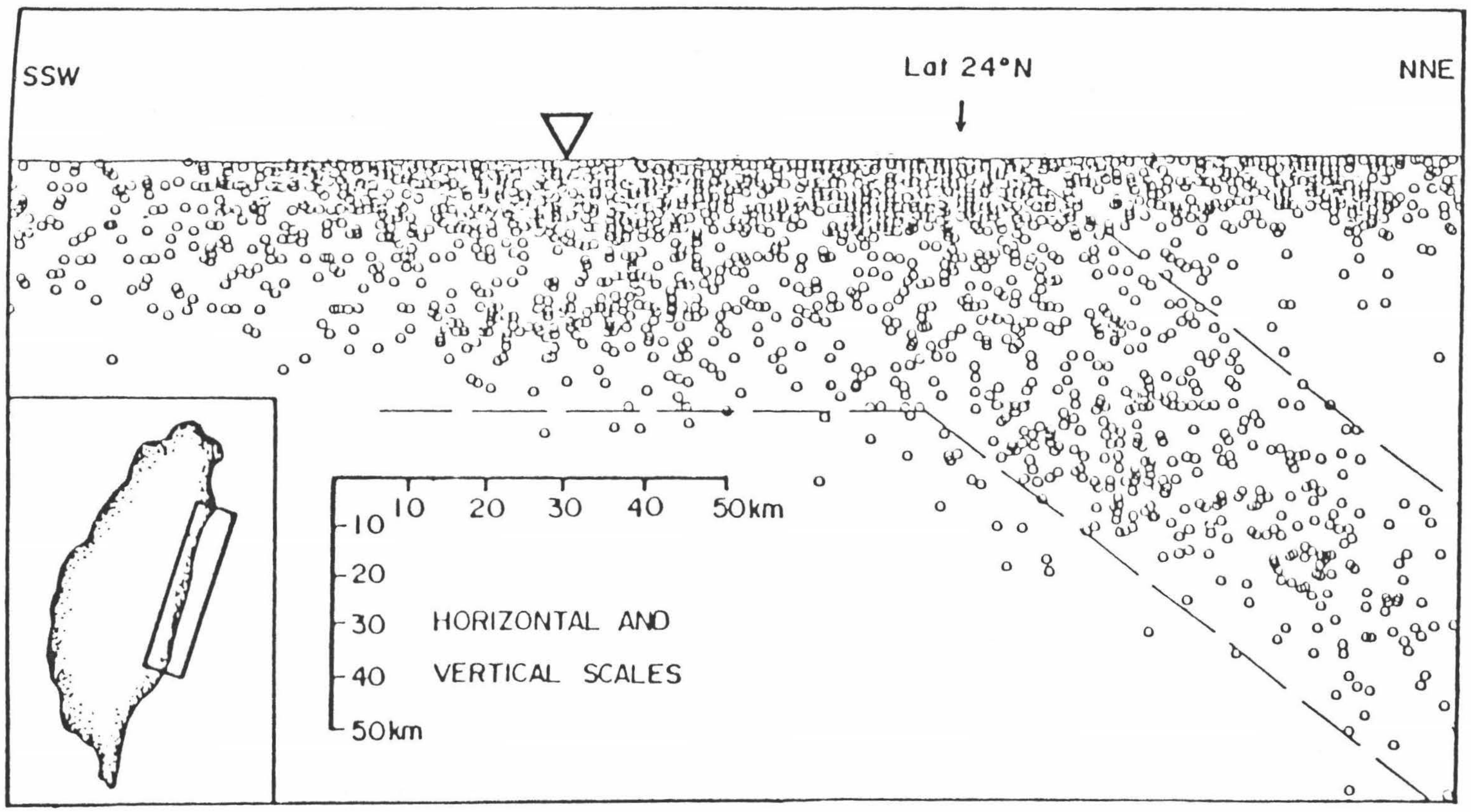
SSW
Lat 24°N
NNE
10 20 30 40 50km
10
20
30
40
50km
HORIZONTAL AND
VERTICAL SCALES

CONCLUSIONS

The results of this study show that off southern and central Taiwan the crust is oceanic. The crust was found to be about 8 km thick in this area and it can be modeled by several layers with velocities and thicknesses that lie within the range associated with "normal" oceanic crust. Near 23.5° N a downwarping and thickening of the low-velocity layers occurs. Immediately to the north of this downwarping, the bottom shoals rapidly onto the continental shelf of the Asian mainland. We believe that this thickened trough of low-velocity materials may represent the sediment filled axis of the Ryukyu Trench. If this is true, it indicates a more southerly trench position in this area than had been previously thought.

A southerly trench position is supported by the gravity data of Bowin et al. (1978) which indicates that the Ryukyu Trench is continuous near Taiwan and not offset to the north by a transform as hypothesized by Wu (1970, 1978). Seismicity profiles perpendicular to the arc, using data from both WWSN and TTSN, were examined in an attempt to shed more light on this problem. However, because of inherent problems with the resolution of both data sets, the results are ambiguous and cannot be used to resolve this question.

APPENDIX A

TAIWAN OBS EXPERIMENT (TOE 1985)
OBS LOCATIONS

OBS	LATITUDE	LONGITUDE	DEPTH (M)
TS(224)	25.0713	122.5043	1300
E(225)	24.8600	122.7200	1500
Q(226)	24.5300	122.2600	370
Z(227)	24.2400	122.5050	900
C(228)	24.1480	122.0540	3130
Y(229)	24.0580	122.6150	3660
JM(230)	23.6000	122.1520	3200
U(231)	23.5245	121.8477	1520
DV(232)	23.2350	122.3500	2160
A(233)	23.1390	121.6840	2240

Deployment period: J.D. 169 - 201, 1985.

APPENDIX B

TOE 1985 EXPLOSIVE SHOT DATA

SHOT #	GMT	LAT	LONG	SIZE KG.	DEPTH M	WATER DEPTH
01	000 00:00:00.000	24.9367	122.7193	005	050	1450
02	198 23:55:03.524	24.8081	122.6411	005	050	1350
03	199 01:06:32.384	24.8075	122.7868	005	050	1530
04	199 04:52:56.934	24.2917	122.5006	025	063	0370
05	199 07:48:02.959	24.2345	122.3980	100	082	1050
06	199 08:32:28.116	24.1811	122.4588	005	050	1100
07	199 09:30:25.806	24.2303	122.5539	006	054	0875
08	199 10:29:49.329	24.1303	122.6169	005	050	1920
13	199 21:24:25.942	23.2114	122.3841	005	050	2350
14	199 22:01:35.353	23.2182	122.3018	005	050	2140
15	199 22:40:24.224	23.2735	122.3452	005	050	2130
16	199 23:30:37.650	23.3441	122.2890	100	082	0000
17	200 00:37:11.993	23.4778	122.2439	100	082	0000
18	200 01:32:24.524	23.5428	122.1404	005	050	4440
19	200 02:08:26.251	23.6179	122.0982	005	050	3400
20	200 02:50:51.883	23.6294	122.1899	100	082	3500
21	200 04:14:01.384	23.7416	122.1387	225	100	2850
22	000 00:00:00.000	23.9092	122.0732	225	100	0000
11	000 00:00:00.000	24.0874	122.3671	225	103	2940
09	200 21:24:58.662	23.9973	122.6685	005	050	3670
10	200 22:14:46.575	24.0580	122.5471	005	050	3410
12	201 00:07:27.696	24.1062	122.2178	225	103	2720
33	201 01:41:33.010	24.1219	122.0420	250	103	3280
23	201 03:03:54.939	24.1461	121.8628	225	103	1780
24	201 04:12:20.882	24.2575	121.9325	225	103	3000
32	201 05:26:28.816	24.2359	122.1026	100	088	3000
31	201 06:08:35.913	24.3256	122.1599	100	080	2350
30	201 06:55:31.301	24.4173	122.2185	100	080	1000
29	201 08:12:35.361	24.6234	122.3156	050	050	0150
28	201 08:56:59.224	24.7303	122.3533	050	050	1025
27	201 09:53:23.839	24.8411	122.4049	050	050	1753
26	201 10:49:04.647	24.9601	122.4529	050	050	1470
34	201 21:30:57.126	23.9965	121.9995	225	103	2400
35	201 22:49:22.489	23.8485	121.9605	225	103	3160
36	201 23:47:51.188	23.7634	121.9221	225	103	2870
37	202 01:07:53.623	23.6393	121.8786	200	094	0000
37A	202 02:58:24.813	23.5630	121.8036	005	002	4200
40	202 05:43:09.049	23.2960	121.7347	100	088	2150
38	202 08:06:46.578	23.4495	121.8120	100	088	0000
42	202 09:34:57.358	23.0035	121.6160	100	088	2380

APPENDIX C

Figure 22

OBS A raytrace through the final model of this study.

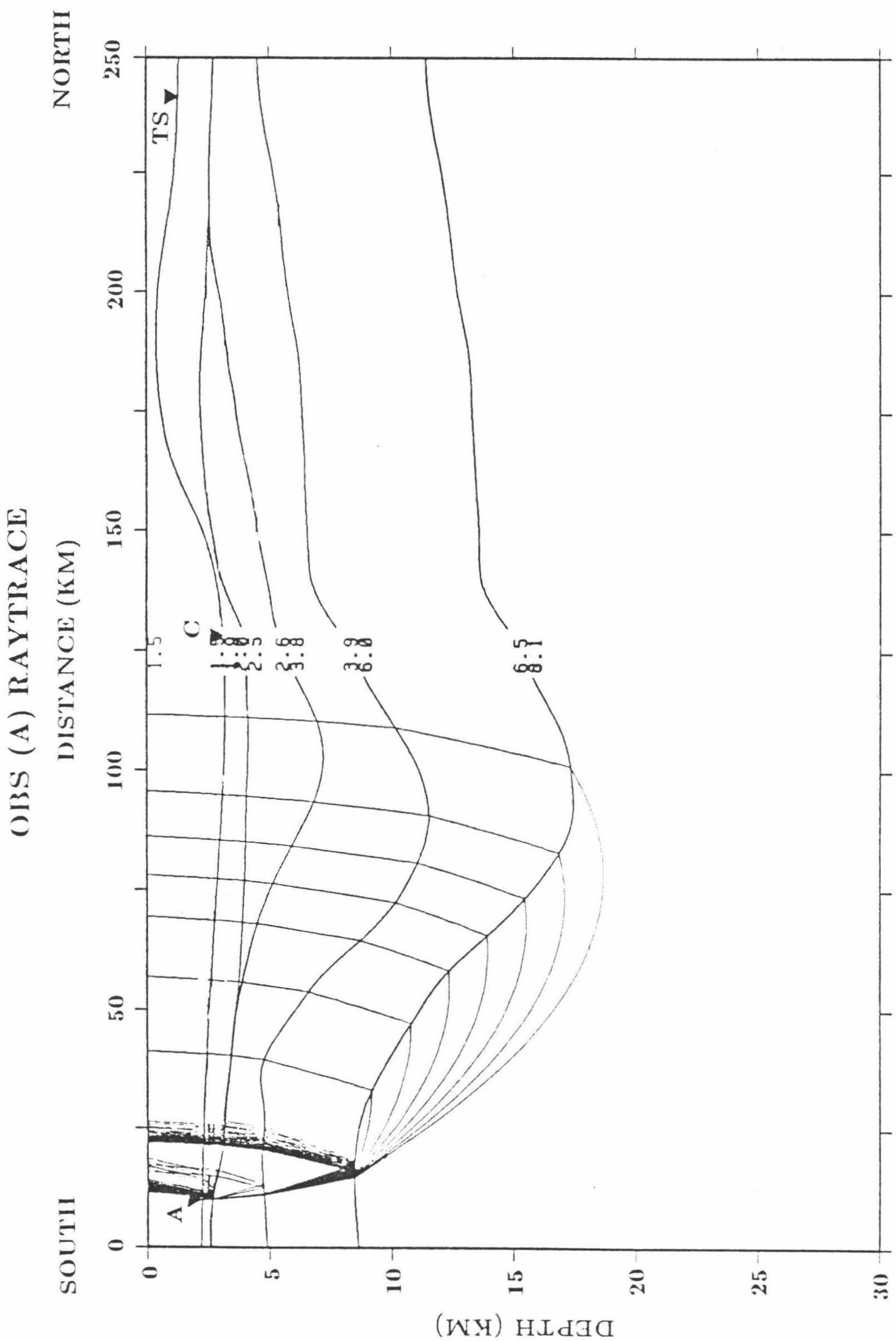
OBS (A) RAYTRACE
DISTANCE (KM)
DEPTH (KM)
SOUTH
NORTH
0
50
100
150
200
250
0
5
10
15
20
25
30
TS
A
C
1.5
2.6
3.8
6.5
8.1

Figure 23

OBS C raytrace through the final model of this study.

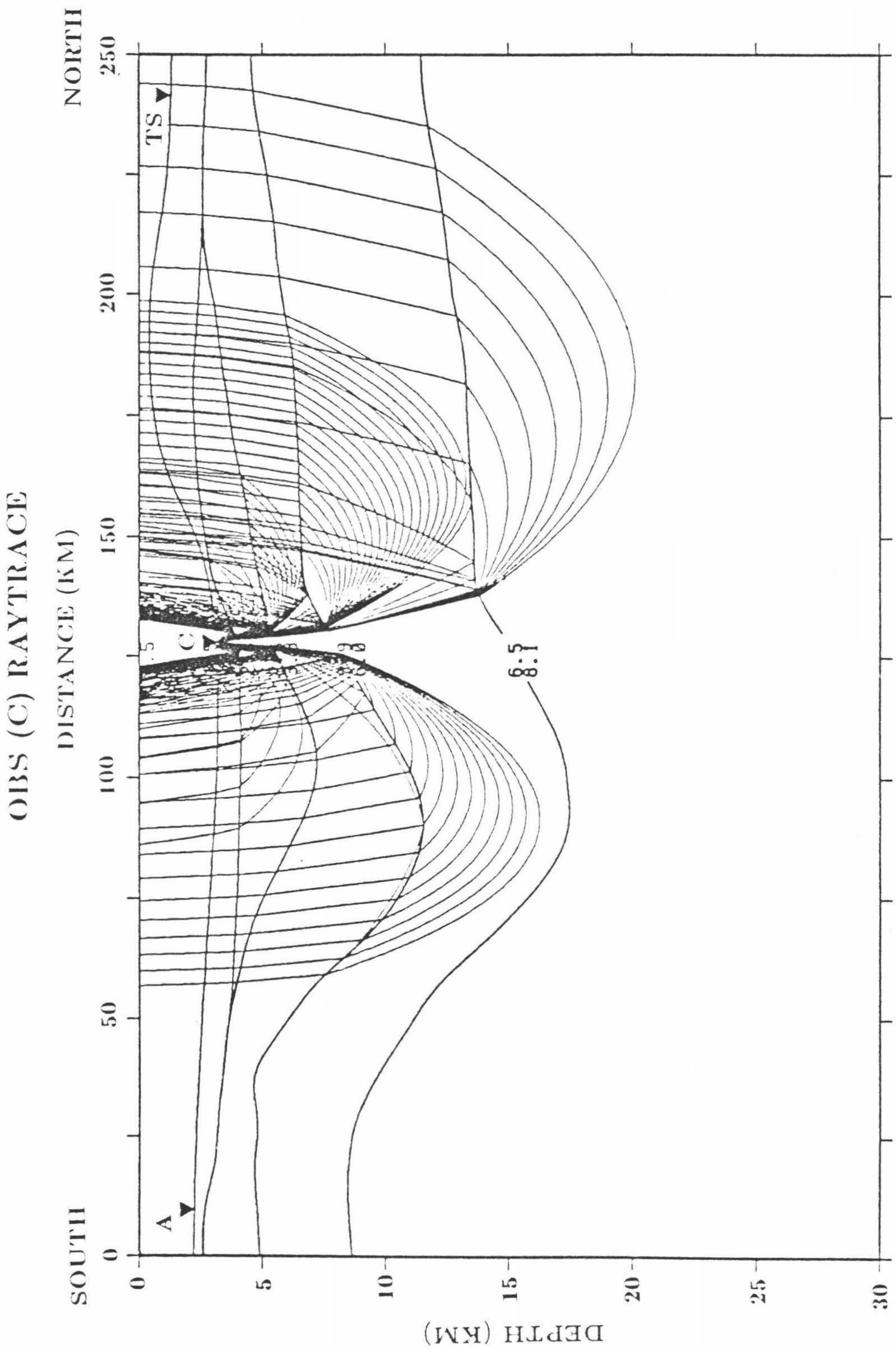
OBS (C) RAYTRACE
DISTANCE (KM)
DEPTH (KM)
SOUTH
NORTH
TS
A
C
6.5
8.1

Figure 24

OBS TS raytrace through the final model of this study.

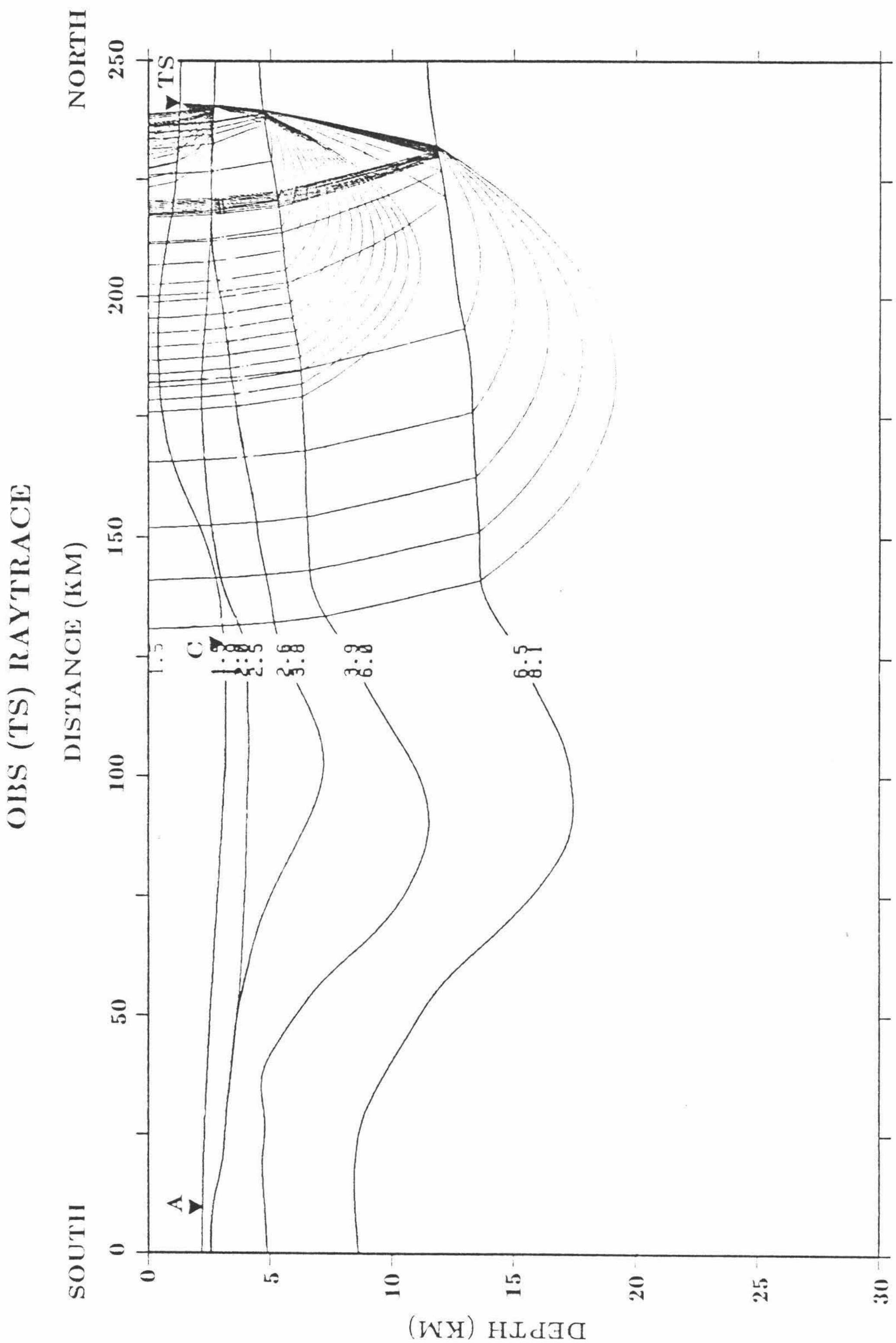
OBS (TS) RAYTRACE
DISTANCE (KM)
DEPTH (KM)
SOUTH
NORTH
TS
A
C
0
50
100
150
200
250
5
10
15
20
25
30
2.6
3.8
3.9
6.5
8.1

REFERENCES

Biq, C., 1981, Collision, Taiwan-style, Mem. Geol. Soc. China, 4, 91-102.

Bowin, C., Lu, R.S., Lee, C.S., and Schouten,H., (1978), Plate convergence and accretion in Taiwan-Luzon region, AAPG Bull., 62, 1645-1672.

Byrne, D.A., Sutton, G.H., Blackington, J.G., and Duennebier, F.K., (1983), Isolated sensor ocean bottom seismometer, Mar. Geophys. Res., 5, 437-449.

Cardwell, R.K., Isacks, B.L., and Karig, D.E., 1980, The spatial distribution of earthquakes, focal mechanisms solutions, and subducted lithosphere in the Philippine and northeastern Indonesian islands, in The Tectonic and Geologic Evolution of Southeast Asian Seas and Islands, Geophys. Monogr. Ser. 23 , edited by D.E. Hayes, 1 - 35, AGU, Washington, D.C., 1980.

Chai, B.H.T., (1972), Structure and tectonic evolution of Taiwan, Am. Jour. Sci., 272, 389-422.

Christensen, N.I., and Salisbury, M.H., 1975, Structure and composition of the lower oceanic crust, Rev. Geophys. Space Phys., 13, 57-86.

Clague, D.A., and Straley, P.F., 1977, Petrologic nature of the oceanic Moho, Geology, 5, 133-136.

Ernst, W.G., Ho, C.S., and Liou, J.G., 1985, Rifting, drifting, and crustal accretion in the Taiwan sector of the Asian continental margin, in Tectonostratigraphic Terranes of the Circum-Pacific Region, AAPG Spec. Vol., edited by D.G. Howell,375-389

Fitch, T.J., (1972), Plate convergence, transcurrent faults, and internal deformation adjacent to Southeast Asia and the Western Pacific, J. Geophys. Res., 77, 4432-4460.

Gebrande, H., (1976), A seismic-ray tracing method for two-dimensional inhomogeneous media, in Explosion Seismology in Central Europe: Data and Results, edited by Giese, Prodehl, and Stein, Springer-Verlag, New York, 1976.

Hamburger, M.W., Cardwell, R.K., and Isacks, B.L., (1983), Seismotectonics of the northern Philippine island arc, in The Tectonic and Geologic Evolution of Southeast Asian Seas and Islands, Geophys. Monogr. Ser. 27, edited by D.E. Hayes, 1-22, AGU, Washington, D.C., 1983.

Ho, C.S., (1976), Foothills tectonics of Taiwan, Bull. Geol. Surv. Taiwan, 25, 9-28.

Ho, C.S., (1986), A synthesis of the geologic evolution of Taiwan, Tectonophysics, 125, 1-16.

Houtz, R., and Ewing, J., 1976, Upper crustal structure as a function of plate age, J. Geophys. Res., 81, 2490 - 2498.

Hsu, T.L., (1962), Recent faulting in the Longitudinal Valley of eastern Taiwan, Mem. Geol. Soc. China, 1, 95-102.

Hsu, V., Wang, C., and Liaw, C.S., (1986), Aftershocks recorded by a land stations and ocean bottom seismometers joint array northeast of Taiwan, (abstract) in Eos, 67, 1085.

Juan, V.C., (1975), Tectonic evolution of Taiwan, Tectonophysics, 26, 197-212.

Juan, V.C., Lo, H.J., and Chen, C.H., (1983), Geotectonics of Taiwan - An overview, in Geodynamics of the western Pacific-Indonesian region, edited by T.W.C. Hilde and S. Uyeda, AGU Geodynamics Series, 11, 379-386.

Karig, D.E., (1973), Plate convergence between the Philippines and the Ryukyu Islands, Marine Geol., 14, 153-168

Katsumata, M., and Sykes, L.R., (1969), Seismicity and tectonics of the western Pacific: Izu-Mariana-Caroline and Ryukyu-Taiwan regions, J. Geophys. Res., 74, 5923-5948.

Kimura, M., (1985), Formation of the Okinawa Trough, in Formation of Active Ocean Margins, edited by N. Nasu et.al., p. 567-591, Terrapub, Tokyo, 1985.

Lee, C.S., Shor, G.G., Bibee, L.D., Lee, R.S., and Hilde, T.W.C., (1980), Okinawa Trough: origin of a back-arc basin, Marine Geol., 35, 219-241.

Lee, T.Q., (1983), Focal mechanism solutions and their tectonic implications in Taiwan region, Bull. Inst. Earth Sci. Academia Sinica, 3, 37-54.

Letouzey, J., and Kimura, M., (1985), Okinawa Trough genesis: structure and evolution of a back-arc basin developed in a continent, Marine Pet. Geol., 2, 111-130.

Leyden, R., Ewing, M., and Murauchi, S., (1973), Sonobuoy refraction measurements in East China Sea, AAPG Bull., 57, 2396-2403.

Lewis, S.D., and Hayes, D.E., 1983, The tectonics of northward propagating subduction along eastern Luzon, Philippine Islands, in The Tectonic and Geologic Evolution of Southeast Asian Seas and Islands, Geophys. Monogr. Ser. 27, edited by D.E. Hayes, 57 - 78, AGU, Washington, D.C., 1983.

Lin, M.T., and Tsai, Y.B., (1981), Seismotectonics in Taiwan-Luzon area, Bull. Inst. Earth Sci. Academia Sinica, 1, 51-82.

Lu, R.S., Lee, C.S., and Kuo, S.Y., (1977), An isopach map for the offshore area of Taiwan and Luzon, Acta Oceanographica Taiwanica, 7, 1-9.

Ludwig, W.J., Murauchi, S., Den, N., Buhl, P., Hotta, H., Ewing, M., Asanuma, T., Yoshii, T., and Sakajiri, N., (1973), Structure of East China Sea-West Philippine Sea margin off southern Kyushu, Japan, J. Geophys. Res., 78, 2526-2536.

Menard, H.W., and Chase, T.E., 1978, Bathymetric Atlas of the North Pacific Ocean, compiled by Scripps Institute of Oceanography, for the Naval Oceanographic Office, NSTL Station, Bay St. Louis, MS, 1978.

Mrozowski, C.L., Lewis, S.D., and Hayes, D.E., 1982, Complexities in the tectonic evolution of the West Philippine Basin, Tectonophysics, 82, 1 - 24.

Murauchi, S., Den, N., Asano, S., Hotta, H., Yoshii, T., Asanuma, T., Hagiwara, K., Ichikawa, K., Sato, T., Ludwig, W.J., Ewing, J.I., Edgar, N.T., and Houtz, R.E., (1968), Crustal structure of the Philippine Sea, J. Geophys. Res., 73, 3143-3171.

Seno, T., (1977), The instantaneous rotation vector of the Philippine Sea plate relative to the Eurasian plate, Tectonophysics, 42, 209-226.

Seno, T., and Kurita, K., (1978), Focal mechanisms and tectonics in the Taiwan-Philippine region, in Geodynamics of the Western Pacific, J. Phys. Earth Suppl. Issue, edited by Uyeda, Murphy, and Kobayashi, 249-263.

Sinton, J.B., (1982), Detailed geophysical studies of two-dimensional structures at active plate margins using seismic refraction and earthquake data, Ph.D Dissertation, University of Hawaii, 1982.

Suppe, J., (1984), Kinematics of arc-continent collision, flipping of subduction, and back-arc spreading near Taiwan, Memoir Geol. Soc. China, 6, 21-33.

Suppe, J., (1981), Mechanics of mountain building and metamorphism in Taiwan, Memoir Geol. Soc. China, 4, 67-89.

Sutton, G.H., Kasahara, J., Ichinose, W., and Byrne, D., (1977), Ocean bottom seismometer development at the Hawaii Institute of Geophysics, Marine Geophys., 3, 153-177.

Taylor, B., and Hayes, D.E., 1983, Origin and history of the South China Basin, in The Tectonic and Geologic Evolution of Southeast Asian Seas and Islands, Geophys. Monogr. Ser. 27, edited by D.E. Hayes, 23 - 56, AGU, Washington, D.C., 1983.

Tsai, Y.B., Teng, T.L., Chiu, J.M., and Liu, H.L., (1977), Tectonic implications of the seismicity in the Taiwan region, Memoir Geol. Soc. China, 2, 13-41.

Wu, F.T., (1978), Recent tectonics of Taiwan, J. Phys. Earth (suppl.), 26, 265-299.

Wu, F.T., (1970), Focal mechanisms and tectonics in the vicinity of Taiwan, Bull. Seismol. Soc. Am., 60, 2045-2056.